iScience

CellPress
OPEN ACCESS

Article

Leishmania major centrin knock-out parasites reprogram tryptophan metabolism to induce a pro-inflammatory response

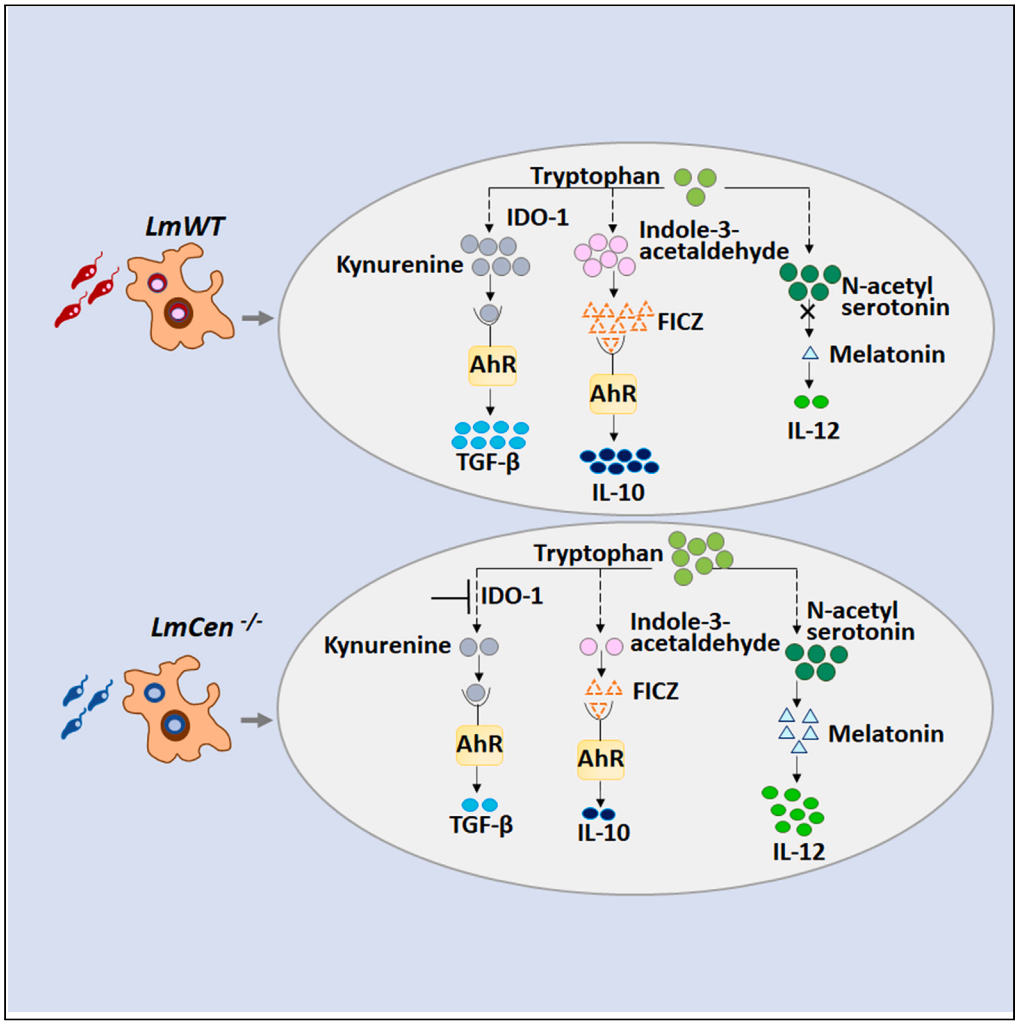

Timur Oljuskin, Nazli Azodi, Greta Volpedo, ..., Abhay R. Satoskar, Sreenivas Gannavaram, Hira L. Nakhasi

sreenivas.gannavaram@fda.hhs.gov (S.G.)
hira.nakhasi@fda.hhs.gov (H.L.N.)

Highlights

Tryptophan metabolism is differentially regulated in *LmWT* and *LmCen*$^{-/-}$ infections

LmCen$^{-/-}$ infection uses tryptophan for the synthesis of TNF-α-promoting melatonin

LmCen$^{-/-}$ infection downregulates kynurenine, a product of tryptophan metabolism

LmWT infection produces kynurenine that promotes anti-inflammatory activities

Oljuskin et al., iScience 26, 107593
September 15, 2023
https://doi.org/10.1016/j.isci.2023.107593

iScience

CellPress
OPEN ACCESS

Article

Leishmania major centrin knock-out parasites reprogram tryptophan metabolism to induce a pro-inflammatory response

Timur Oljuskin,[1,8] Nazli Azodi,[2,8] Greta Volpedo,[3] Parna Bhattacharya,[2] Hannah L. Markle,[2] Shinjiro Hamano,[4,5] Greg Matlashewski,[6] Abhay R. Satoskar,[3,7] Sreenivas Gannavaram,[2,9,*] and Hira L. Nakhasi[2,*]

SUMMARY

Leishmaniasis is a parasitic disease that is prevalent in 90 countries, and yet no licensed human vaccine exists against it. Toward control of leishmaniasis, we have developed *Leishmania major centrin* gene deletion mutant strains (*LmCen*$^{-/-}$) as a live attenuated vaccine, which induces a strong IFN-γ-mediated protection to the host. However, the immune mechanisms of such protection remain to be understood. Metabolomic reprogramming of the host cells following *Leishmania* infection has been shown to play a critical role in pathogenicity and shaping the immune response following infection. Here, we applied untargeted mass spectrometric analysis to study the metabolic changes induced by infection with *LmCen*$^{-/-}$ and compared those with virulent *L. major* parasite infection to identify the immune mechanism of protection. Our data show that immunization with *LmCen*$^{-/-}$ parasites, in contrast to virulent *L. major* infection promotes a pro-inflammatory response by utilizing tryptophan to produce melatonin and downregulate anti-inflammatory kynurenine-AhR and FICZ-AhR signaling.

INTRODUCTION

Leishmaniasis is a parasitic disease caused by the various strains of the blood-borne protozoan species *Leishmania*, which is transmitted to humans via the bite of an infected sandfly. The disease pathology ranges from localized skin ulcers (cutaneous leishmaniasis, CL) disfiguring scars (mucocutaneous leishmaniasis, MCL) to often fatal systemic disease (visceral leishmaniasis, VL), depending on the species of the *Leishmania* parasite. CL is the most prevalent form of the disease, which is commonly caused by *Leishmania major* in the Old World and *Leishmania mexicana* in the Americas.[1–3] Approximately, one billion people are at risk of infection, mainly in tropical and subtropical countries, and autochthonous infections have been reported in the southern regions of the United States[4]; however, no licensed vaccines currently exist, and treatment options remain limited.[1,2]

Toward the control of leishmaniasis, our group has previously developed a genetically modified *L. major* mutant strain where the *centrin* gene was deleted (*LmCen*$^{-/-}$) via CRISPR/cas-9 technology.[5] Previous studies showed that deletion of centrin from *L. donovani* results in a significant growth defect in the amastigote form of the parasite and loss of virulence.[6] Immunization with centrin deleted *L. donovani* protected hosts against virulent challenge in studies with mice, hamsters, and dogs.[7,8] The deletion of the *centrin* gene from *L. major* similarly caused a loss of virulence that resulted in a lack of skin lesions and gradual clearance of *LmCen*$^{-/-}$ parasites from the host.[5] Immunization with the *LmCen*$^{-/-}$ parasites induced a strong Th1response in the hosts and protected them against challenge by the virulent *L. major* or *L. donovani* strains.[5,9]

Several experimental *Leishmania* vaccines have been tested in pre-clinical models and a few have advanced to clinical trials.[10] However, the immune mechanisms of protection beyond those involved in the induction of Th1 immunity remain to be explored. It has been shown that *L. major* parasites can interfere with the host's immune signaling pathways in favor of their growth and immune evasion.[11–13] For example, IFN-γ production is critical for the destruction of intracellular parasites through the induction of nitric oxide, superoxide anions, and GTPases.[14,15] Persistence of *Leishmania* parasites in the host is strongly dependent on the inhibition of IFN-γ production, the induction of the anti-inflammatory IL-10 and an elevated level of TGF-β that inhibit anti-microbial macrophage functions.[1,16–19] On the other hand, previous work showed

[1]Animal Parasitic Diseases Laboratory, Agricultural Research Service, USDA, Beltsville, MD 20705, USA
[2]Division of Emerging and Transfusion Transmitted Diseases, CBER, FDA, Silver Spring, MD 20993, USA
[3]Department of Microbiology, The Ohio State University, Columbus, OH 43210, USA
[4]Department of Parasitology, Institute of Tropical Medicine (NEKKEN), The Joint Usage/Research Center on Tropical Disease, Nagasaki University, Nagasaki, Japan
[5]Nagasaki University Graduate School of Biomedical Sciences Doctoral Leadership Program, Nagasaki, Japan
[6]Department of Microbiology and Immunology, McGill University, Montreal, QC, Canada
[7]Department of Pathology, Wexner Medical Center, The Ohio State University, Columbus, OH 43210, USA
[8]These authors contributed equally
[9]Lead contact
*Correspondence: sreenivas.gannavaram@fda.hhs.gov (S.G.), hira.nakhasi@fda.hhs.gov (H.L.N.)
https://doi.org/10.1016/j.isci.2023.107593

that immunization with the *LmCen*$^{-/-}$ strain significantly increases the pro-inflammatory Th1 response following challenge with either virulent *L. major* or *L. donovani*, indicated by the presence of IFN-γ producing effector T-cells, and elevated IFN-γ/IL-10 ratios analogous to leishmanization.[9,5] In contrast, another *centrin* deletion mutant in *L. mexicana* background also conferred protection against challenge with either *L. mexicana* or *L. donovani* in the immunized hosts by downregulating IL-10 response, while the IFN-γ mediated Th1 response remained unchanged between the naive and immunized groups[21,22] The immune mechanisms of protection thus appear to be different in *LmCen*$^{-/-}$ and *LmexCen*$^{-/-}$ strains.

While pathogenicity characteristics are typically addressed from an immunological perspective, numerous studies have highlighted the importance of metabolomic reprogramming in disease development.[23–26] In *Leishmania* infection, early differentiation of macrophages into M1 and M2 states, and the associated immune response that either favors the host or the parasite respectively, is driven by metabolic changes.[13,27,28] Such metabolic reprogramming occurs prior to the onset of an immune response, highlighting the role of metabolic products as ligands for transcription factors that turn on the expression of cytokines and other immune factors.[29] Increased levels of glutaminolysis and oxidative phosphorylation have been shown to determine the activation status of plasmacytoid DCs.[30,31] Increased fatty acid oxidation or glycolysis causes TLR4 mediated DC activation, demonstrating the role of metabolic changes in shaping innate immune responses.[32,33] Both gluconeogenesis and the pentose phosphate pathway are shown to be necessary for amastigote replication in the macrophages,[27,34–36] where fatty acids[27,37,38] and amino acids[27,39,40] can serve as vital carbon sources for the parasites. Similarly, *L. infantum* parasites manipulate the AMPK pathway to significantly increase the oxidative phosphorylation necessary for amastigote replication.[13]

While these studies have established the role of metabolic programming in *Leishmania* pathogenesis, similar studies addressing the vaccine-mediated immune response in *Leishmania* have not been performed. Studies in viral vaccines such as ΔF/TriAdj, a vaccine against respiratory syncytial virus (RSV, showed that immunization with the attenuated viruses modulates tryptophan metabolism to enrich serotonin levels, while virulent RSV infection causes enrichment of kynurenine and heightened levels of amino acid biosynthesis and the Urea cycle.[41]

We undertook studies to explore the metabolic pathways underlying the immune mechanisms of protection associated with *LmCen*$^{-/-}$ immunization in mice. We chose a 7-day time point based on the literature regarding *Leishmania* infection that showed early T cell responses detectable following APC-T cell interactions.[42] These studies showed that following *L. major* infection, antigen-specific proliferation of CD4^{+} T cells could be detected in the lymph nodes of mice as early as day 3 of infection,[43] indicating that immune-regulatory events that determine the adaptive immune responses start occurring in the initial stages of the infection. An untargeted metabolomics analysis of the ear tissue showed various metabolic pathways were significantly enriched in *LmCen*$^{-/-}$ immunization, which could be driving the immune-protective benefits of the vaccine. Specifically, we discovered that following *LmCen*$^{-/-}$ immunization tryptophan metabolism is reprogrammed which could influence the protective immunity. To our knowledge, this is the first report to explore metabolic drivers of immune response of *L. major* vaccine candidates.

RESULTS

Mass spectrometric analysis of the ear tissue

The ear tissues of mice intradermally inoculated with either *LmWT*, *LmCen*$^{-/-}$, or PBS as a control were used to perform mass spectrometry to identify metabolites and metabolomic pathways associated with the immune mechanisms that underlie infection and immunization (Figure 1A). No differences in the parasitic burden in the ears (Figure 1B) or draining lymph nodes (Figure 1C) were observed that could cause a bias in the metabolic signatures reported herein. A two-way comparison between *LmWT* vs. Naive, *LmCen*$^{-/-}$ vs. Naive, and *LmCen*$^{-/-}$ vs. *LmWT* were performed to identify metabolites associated with the immune mechanism of pathogenesis or protection. The two-way comparison data contained 4610, 5158, and 3676 features, respectively. Volcano plots with a fold change threshold of ±2 and a *p*value threshold of 0.05 were used to identify the significant features in the datasets for both the positive (Figures 1D–1F, upper panel) and the negative (Figures 1D–1F lower panel) modes of the mass spectrometry with the former identifying the protonated and the latter identifying the non-protonated molecules respectively. To visualize the overall structure of the datasets and determine whether unique metabolite signatures exist among the three comparisons, partial least squares discriminant (PLS-DA) analysis, a multivariate dimensionality reduction method, was performed using the data from both positive (Figures 1G–1I, upper panel) and the negative (Figures 1G–1I, lower panel) modes. The PLS-DA clustered the metabolites into three non-overlapping groups with 17.7%–34.7% and 4.6%–8.6% of the variance explained by the first two principal components, respectively, indicating that the three conditions of naive, virulent infection and immunization lead to distinct enrichments.

Arginine metabolism is significantly altered in LmCen−/− immunization compared to LmWT infection

To identify metabolic pathways distinctly enriched in the ear tissues immunized with *LmCen*$^{-/-}$ in comparison to the naive and the *LmWT*-infected mice tissues, both the mummichog and the Gene Set Enrichment Analysis (GSEA) algorithms were used to analyze the positive (Figures 2A–2C) and negative mode datasets (Figures 2D–2F). For this analysis p values were integrated together via a Fisher's method and visualized the results with 'MS Peaks to Pathways' plots. The metabolic pathways enriched in the three different groups were identified through the comparisons of *LmWT* vs. Naive (Figures 2A and 2D), *LmCen*$^{-/-}$ vs. Naive (Figures 2B and 2E), and the *LmWT* infection against the *LmCen*$^{-/-}$ immunization (Figures 2C, 2F, and 2G), indicating the distinct pathways enriched under each condition and also common pathways are shared between *LmWT* and *LmCen*$^{-/-}$ infections (Figure 2G). Results showed that arginine biosynthesis to be one of the most highly enriched pathways in the *LmCen*$^{-/-}$ immunization in comparison to the naive and the *LmWT* infection (highlighted by the black box, Figure 2B). To verify the results, pathway enrichment was also conducted by ingenuity pathway analysis (IPA) to identify the canonical pathways

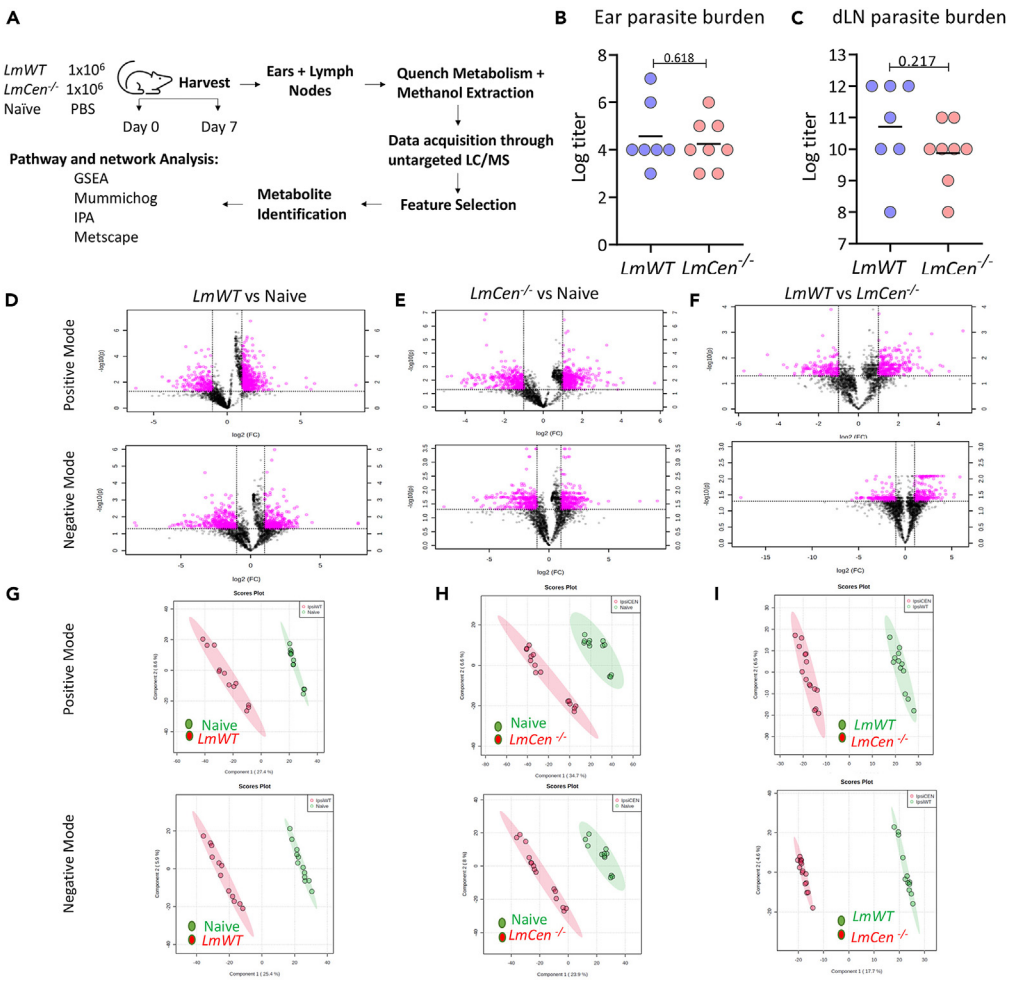

Figure 1. Infection with *LmWT* and immunization with *LmCen*$^{-/-}$ display distinct metabolic signatures at the inoculation site

(A–I) Female C57Bl/6 mice (n = ≥4 per group) were injected intradermally in the ear with stationary phase *LmWT*, *LmCen*$^{-/-}$ parasites. After 7 days, the ear tissues were collected and processed for mass spectrometry. The data acquired was used to identify enriched metabolites and construct activated metabolomic pathways (A). Parasite burdens at day 7 post-infection from ears (B) and draining lymph nodes (C) were measured by limiting dilution. Data are represented as mean ± SEM. Data represents one of three experiments with N = 8 per group. The displayed p value was obtained using an unpaired t test. Normalized data from ear tissue of C57Bl/6 mice was used to perform statistical analysis (D–F). Features selected by volcano plot with <0.05 false-discovery rate (FDR) and > 2-fold change (FC) threshold cutoffs from positive and negative modes for ear tissue of *LmWT* vs. naive, *LmCen*$^{-/-}$ vs. naive, and *LmCen*$^{-/-}$ vs. *LmWT* mice with log-transformed fold change (x) 2 and t-tests thresholds (y) 0.05 (G–I). Partial least squares-discriminant analysis (PLS-DA) from positive and negative mode for ear tissue of *LmWT* vs. naive (G), *LmCen*$^{-/-}$ vs. naive (H), and *LmCen*$^{-/-}$ vs. *LmWT* (I) mice indicating the existence of distinct metabolic signatures under the infection and immunized conditions. LC/MS, liquid chromatography/mass spectrometry; GSEA, gene set enrichment analysis.

(Figure S1). The results from IPA also showed that arginine biosynthesis is one of the most highly enriched pathways in the *LmCen*$^{-/-}$ immunization in comparison to the naive and *LmWT* datasets. Metabolites involved in the arginine biosynthesis pathway detected in the normalized LC/MS outputs and their fold change levels are listed (Table 1). Our data showed that L-arginine is enriched in both the positive mode *LmWT* infection and the *LmCen* $^{-/-}$ immunization in comparison to the naive control. However, the *LmWT* vs. *LmCen*$^{-/-}$ comparison showed that L-arginine is more enriched in the *LmCen*$^{-/-}$ compared to *LmWT* infection (Table 1). Spermine, a downstream product of the arginine metabolism derived from spermidine, appeared only in the *LmCen*$^{-/-}$ dataset but not in *LmWT*. Spermine was highly enriched in both the *LmCen*$^{-/-}$ vs. naive and *LmCen*$^{-/-}$ vs. *LmWT* comparisons (Table 1).

Polyamines that enable parasite proliferation are enriched in the LmWT infection

Arginine and citrulline are metabolites connected in a looped relationship in which citrulline is a byproduct of the nitric oxide production via arginine metabolism, and it can be used in arginine synthesis as well through the ornithine cycle. Accordingly, the results of IPA also showed that citrulline metabolism was highly enriched in the *LmWT* infection in comparison to the naive and the *LmCen*$^{-/-}$ infection (Figure S1).

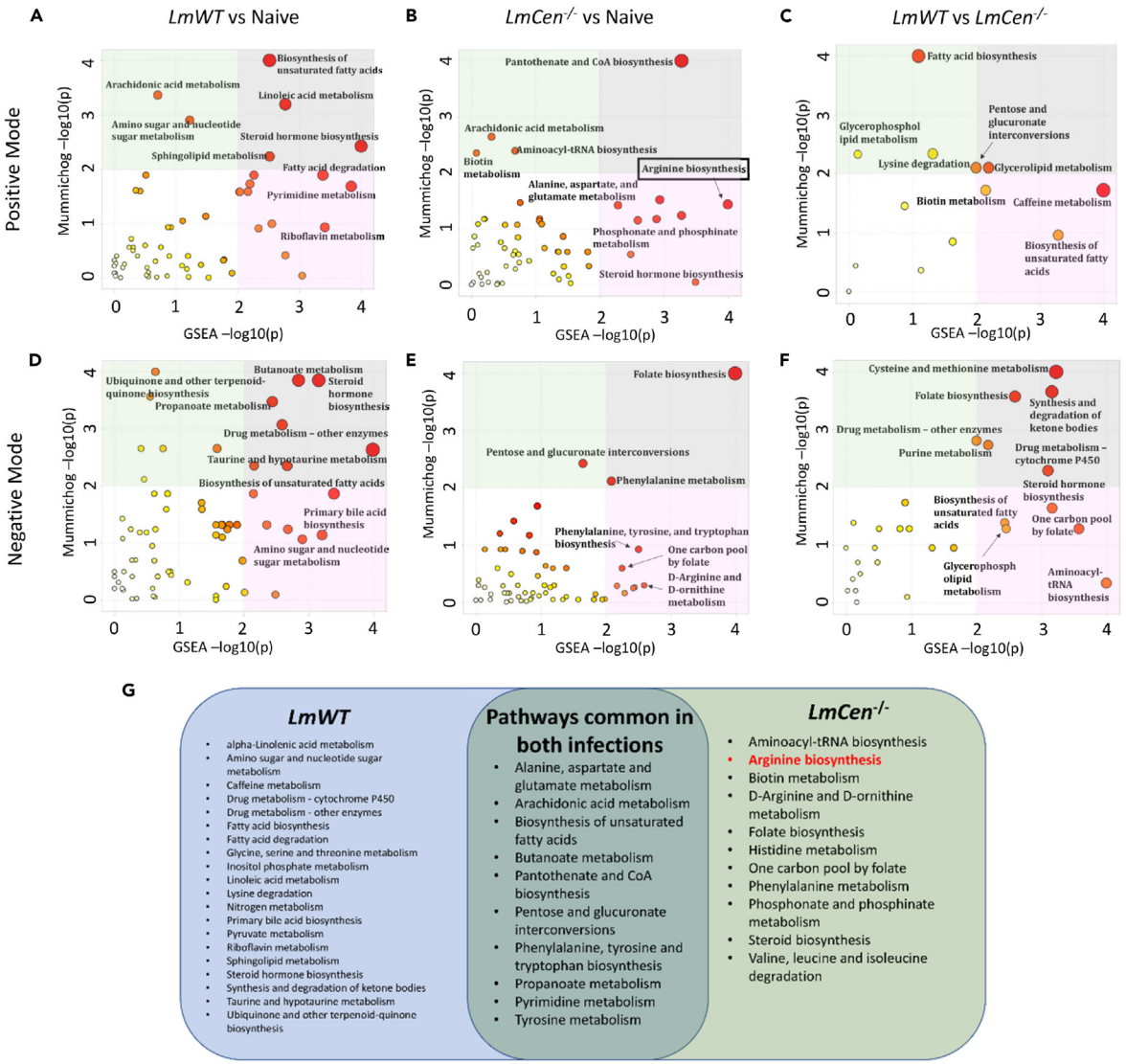

Figure 2. Metabolic pathways enriched in mouse ear tissues infected with *LmWT* or immunized with *LmCen*$^{-/-}$

(A–G) Normalized data from ear tissue of C57Bl/6 mice after 7 days of infection with *LmWT*, immunization with *LmCen*$^{-/-}$ or naive control was used to perform peaks to pathway analysis. Using the MS Peaks to Paths module in MetaboAnalyst5.0, the mummichog and gene set enrichment analysis (GSEA) p values were combined. The Integrated MS Peaks to Paths plot summarizes the results of the Fisher's method for combining mummichog (y) and GSEA (x) p values from the positive (A–C) negative (D–F) mode datasets, indicating the metabolic pathways enriched. The size and color of the circles correspond to their transformed combined p values. Large and red circles are considered the most perturbed pathways. The colored areas show the significant pathways based on either mummichog (green) or GSEA (pink), and the gray area highlights significant pathways identified by both algorithms. Arginine metabolism pathway associated with a protective immune response was found to be enriched in *LmCen*$^{-/-}$ immunization (B, highlighted by the black boxes). A Venn diagram showing the pathways shared between, and uniquely enriched in either of the *LmWT* and *LmCen*$^{-/-}$ infections are shown (G).

Ornithine was exclusively enriched in the *LmWT* vs. naive comparison and was not detected in the *LmCen*$^{-/-}$ vs. naive datasets (Table 1), indicating its importance of polyamines to the parasite proliferation.

Kynurenine levels are altered between LmWT infection and LmCen−/− immunization

Previous studies have shown that tryptophan metabolism is often altered in conjunction with arginine metabolism through the interaction of Arg1 and indoleamine 2,3-dioxygenase 1 (IDO1).[44–46] Tryptophan can be catabolized through the three distinct mechanisms to produce kynurenine, indole, and serotonin (Hsu et al., 2020). In the kynurenine pathway, IDO1 acts as the rate-limiting enzyme in the conversion of the substrate tryptophan into kynurenine and other downstream metabolites such as kynurenic Acid. In the indole pathway, Indole-3-acetaldehyde

Table 1. List of significant metabolites of the arginine metabolism pathway detected by LC/MS and their respective enrichment levels in mice infected with *LmWT* or immunized with *LmCen*$^{-/-}$

Dataset	Compound	m/z Ratio	Log FC
LmWT vs. Naive	L-Arginine	175.120515789341/6.53941666666667	0.711983
	L-Arginine	174.111888273963/12.3793333333333	0.175912
	L-Ornithine	155.079258810298/4.28323333333333	0.777981
	L-Citrulline	198.085631129694/1.26938333333333	0.143353
	L-Citrulline	176.102936662285/1.26938333333333	0.144771
	L-Citrulline	176.1017753953/8.26498333333333	Infinity
	L-Citrulline	351.196228027344/6.74226666666667	−1.53448
	L-Arginine	*347.218973727799/17.9363333333333*	*−0.85208*
	L-Citrulline	*174.087391981391/1.2694*	*0.129864*
	L-Citrulline	*175.094959488147/8.52898333333333*	*1.871527*
LmCen$^{-/-}$ vs. Naive	L-Arginine	175.117476556853/6.35535	0.191052
	L-Citrulline	175.09342956543/14.2167833333333	−0.40031
	L-Citrulline	198.085631129694/1.26938333333333	0.075425
	L-Citrulline	176.102936662285/1.26938333333333	0.064003
	L-Citrulline	351.198661460237/5.61805	−0.17327
	Spermine	241.17788404089/12.7144666666667	0.032859
LmWT vs. *LmCen*$^{-/-}$	L-Arginine	174.111485044507/10.6618166666667	0.413899
	L-Arginine	175.117476556853/6.35535	−0.19811
	L-Citrulline	176.102936662285/1.26938333333333	0.080768
	L-Citrulline	198.085631129694/1.26938333333333	0.067928
	Spermine	241.178182435098/11.1409833333333	−0.20232
	L-Arginine	*209.080528261553/2.07785*	*−0.40848*
	L-Arginine	*347.218973727799/17.9363333333333*	*−0.99784*
	L-Citrulline	*174.087391981391/1.2694*	*0.067751*
	L-Citrulline	*175.094959488147/8.52898333333333*	*1.173381*
	L-Citrulline	*210.065612776268/7.64563333333333*	*Infinity*

Normalized data from ear tissue of C57Bl/6 mice after 7 days of infection with *LmWT*, immunization with *LmCen*$^{-/-}$ or naïve control was used to analyze the concentration levels of metabolites associated with arginine metabolism that were detected in our dataset by mass spectrometry. Different isomers of metabolites could be detected multiples times through various m/z ratios recognized by the mass spectrometry analysis. Metabolites shown in italics were detected by the negative mode LC/MS, while the remainder were detected by the positive mode.

can yield 6-formylindolo[3,2-*b*]carbazole (FICZ), while the serotonin pathway leads to the production of melatonin.[45,47] Kynurenine, FICZ, and melatonin have been shown to have immunoregulatory roles and are of interest in the context of vaccine immunity.

Metabolites associated with the tryptophan metabolism pathway were searched for in the normalized LC/MS outputs to identify their enrichment. As shown in the Table 2, the *LmWT* infection is characterized by a depletion of tryptophan and higher levels of Indole-3-acetaldehyde and one isoform of kynurenine, while two kynurenine isoforms showed a slight downregulation. In contrast, the *LmCen*$^{-/-}$ immunization is distinguished by higher levels of tryptophan, reduced level of Indole-3-acetaldehyde and a downregulation of the kynurenine. Interestingly, melatonin was found highly enriched in the *LmCen*$^{-/-}$ dataset but was undetected in the *LmWT* infection (Table 2).

To better visualize the alterations in tryptophan metabolism, compound-gene network analysis of *LmCen*$^{-/-}$ vs. naive and *LmWT* vs. naive was performed and is shown in Figures 3A and 3B, respectively. This analysis takes into account the variations in the fold changes of isoforms reported in Table 2. Results showed that the tryptophan was detected in both *LmCen*$^{-/-}$ and *LmWT* infections although reduced in the *LmWT* infection, while the products of tryptophan catabolism, i.e., kynurenine and indole-3-acetaldehyde were significantly reduced in *LmCen*$^{-/-}$ immunization compared to *LmWT* infection (Figures 3A and 3B). In contrast, melatonin was enriched in *LmCen*$^{-/-}$ infection but was not detected in *LmWT* infection (Figures 3A and 3B).

Alteration of melatonin levels affect TNF production in LmCen−/− infected BMDCs

Detection of melatonin only in *LmCen*$^{-/-}$ infection prompted us to test whether it could show an adjuvant activity observed in viral vaccine studies.[48–51] To test the hypothesis that melatonin could affect the pro-inflammatory milieu following immunization with *LmCen*$^{-/-}$, supplementation and depletion experiments were performed. 4-Cyano-4-[(dodecylsulfanylthiocarbonyl)sulfanyl]pentanoic acid.

Table 2. List of significant metabolites of the tryptophan pathway detected by LC/MS and their respective enrichment levels in mice infected with *LmWT* or immunized with *LmCen*$^{-/-}$

Dataset	Compound	m/z Ratio	Log FC
LmWT vs. Naive	L-Tryptophan	409.183727323844/16.2527	−0.84285
	Indole-3-acetaldehyde	160.074993175059/8.60266666666667	0.412018
	L-Kynurenine	417.177374622835/6.63973333333333	−0.5874
		209.091836598665/3.50861666666667	−0.08652
		209.094131469727/3.25915	0.354958
LmCen $^{-/-}$ vs. Naive	L-Tryptophan	205.098835651367/1.6815	0.202931025
	Indole-3-acetaldehyde	160.075205801606/4.96223333333333	0.106710051
		160.075511683185/7.90605	0.250066463
	L-Kynurenine	417.177374622835/6.63973333333333	−0.715094839
	Melatonin	232.120675751645/6.94911666666667	6.138261
	Kynurenic Acid	190.049071881504/7.86811666666667	Infinity
LmWT vs. *LmCen* $^{-/-}$	L-Tryptophan	205.098835651367/1.6815	−0.52385
		204.08733700045/14.1969	Infinity
		205.097443451686/4.99411666666667	−0.07056
	Indole-3-acetaldehyde	160.075205801606/4.96223333333333	−0.08637
	L-Kynurenine	209.091836598665/3.50861666666667	−0.15887
		417.177401765291/5.18043333333333	−0.27253

Normalized data from ear tissue of C57Bl/6 mice after 7 days of infection with *LmWT*, immunization with *LmCen*$^{-/-}$ or naïve control was used to analyze the concentration levels of metabolites associated with tryptophan metabolism pathway that were detected in our dataset by mass spectrometry. Different isomers of metabolites could be detected multiples times through various m/z ratios recognized by the mass spectrometry analysis.

(4-CDP), an inhibitor of tryptophan hydroxylases (TPH1 and TPH2), the rate-limiting enzymes in the serotonin pathway, was used to deplete the production of melatonin in naive, *LmWT* and *LmCen*$^{-/-}$ infected BMDCs (Figure 4A). Gene expression levels of TNF and IL-12 were measured following exogenous addition or depletion of melatonin using RT-PCR (Figures 4B–4E). The results show that depletion of melatonin results in significant reduction in TNF in both *LmWT* and *LmCen*$^{-/-}$ infection compared to naive controls, however the reduction in TNF was significantly more in *LmCen*$^{-/-}$ compared to *LmWT* infection. (Figure 4B). The IL-12 levels remained unaltered in both *LmWT* and *LmCen*$^{-/-}$ infections compared to naive controls (Figure 4C). Consistent with this result, addition of melatonin resulted in an increase of both TNF and IL-12 gene expression levels in the *LmWT* and *LmCen*$^{-/-}$ infections (Figures 4D and 4E) in comparison to the naive control.

Inhibition of kynurenine-AhR signaling by 1-methyl tryptophan increases the expression of AhR and IFN-γ

Kynurenine has been well-established in playing an immunomodulatory role through its activity as a ligand for the aryl hydrocarbon receptor (AhR).[52] The high abundance of kynurenine found in *LmWT* infection may thus predispose the infected cells to produce TGF-β and other anti-inflammatory cytokines.[53] To test the hypothesis that the interaction between kynurenine and AhR played a significant role in the immunity of *LmCen*$^{-/-}$, 1-methyl tryptophan (1-MT), a well-characterized IDO-1 inhibitor,[54] was used to deplete the production of kynurenine in naive, *LmWT* and *LmCen*$^{-/-}$ infected BMDCs (Figure 5A). Gene expression levels of IDO-1, AhR, and IFN-γ were measured following IDO-1 inhibition using RT-PCR (Figures 5B–5D). The results showed that the gene expression levels of IDO-1 and AhR are detected at a higher level in the *LmWT* and *LmCen*$^{-/-}$ infections in comparison to the naive treated DCs. IFN-γ levels also increased in *LmWT* and *LmCen*$^{-/-}$ infections compared to naive treated DCs, however the increase was significant in *LmWT* group compared to *LmCen*$^{-/-}$ reflecting the different underlying levels of kynurenine in the two infections (Figure 5D).

Addition of kynurenine decreased the expression of Ido-1, AhR and IFN-γ

The AhR-kynurenine interaction induces the increased transcription of the anti-inflammatory TGF-β, and in turn reduced IFN-γ expression. To confirm that the Kyn-AhR interaction alters IFN-γ gene expression by the levels of kynurenine, we performed *in vitro* experiment in which L-kynurenine was exogenously added to naive, *LmWT* and *LmCen* $^{-/-}$ infected BMDCs (Figure 5A), after which the gene expression levels of IDO-1, AhR and IFN-γ were measured via RT-PCR. The results showed that exogenous addition of kynurenine resulted in a reduced expression of IDO-1, and AhR in the *LmCen*$^{-/-}$ and *LmWT* infected BMDC cultures (Figures 5E and 5F) compared to naive treated DCs. IFN-γ levels also decreased in *LmWT* and *LmCen*$^{-/-}$ infections compared to naive treated DCs, however the reduction was significant in *LmCen*$^{-/-}$ group compared to *LmWT* reflecting the different underlying levels of kynurenine in the two infections (Figure 5G).

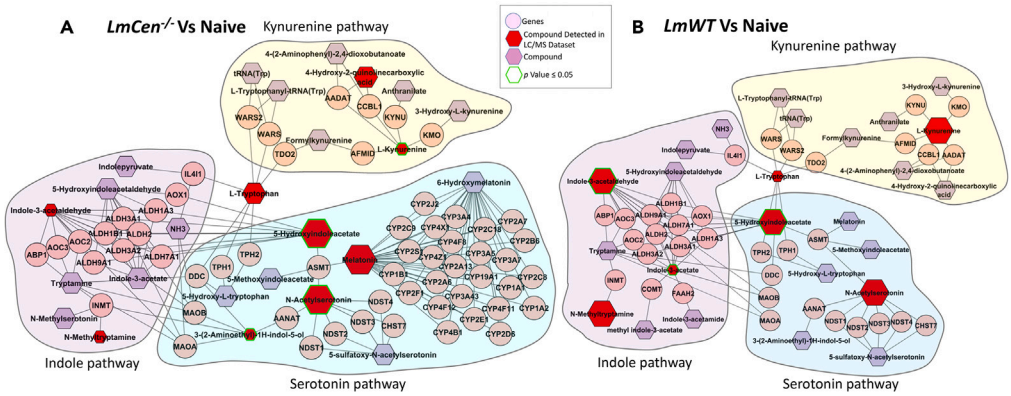

Figure 3. Infection with *LmWT and LmCen*$^{-/-}$ lead to differential regulation of the tryptophan metabolism pathway

(A and B) Normalized data from the ear tissue of C57Bl/6 mice infected with *LmWT*, immunized with *LmCen*$^{-/-}$ and naive controls was used to perform integrative compound-compound network analysis with Metscape. The differential regulation of the tryptophan metabolites, specifically kynurenine, indole-3-acetaldehyde, and melatonin are illustrated in this graph for the immunized (A) and infected (B) conditions compared to naive control. Larger hexagons represent up-regulation, while smaller hexagons represent down-regulation. Red hexagons represent compounds detected in the dataset, while hexagons with a green outline represent statistically significant metabolites (p value $\leq$0.05). The purple hexagons represent compounds that are associated with the pathway but are not detected in the input dataset. The pink circles represent the genes regulating the biosynthetic activities. The networks associated with the kynurenine, indole, and serotonin pathways are highlighted with yellow, purple, and blue hues respectively.

Addition of FICZ elevated the expression of IL-10 and AhR

The AhR-FICZ interaction induces an increased transcription of the regulatory cytokine IL-10. To confirm that the FICZ-AhR interaction alters IL-10 gene expression by the levels of 3-indole acetaldehyde, we performed *in vitro* experiment in which FICZ was exogenously added to naive, *LmWT* and *LmCen* $^{-/-}$ infected BMDCs (Figure 5H), after which the gene expression levels of IL-10 and AhR were measured via RT-PCR. The results showed that exogenous addition of FICZ resulted in an elevated expression of IL-10 and AhR in both *LmCen*$^{-/-}$ and *LmWT* infected BMDC cultures compared to naive treated DCs (Figures 5I and 5J). Upon *LmWT* infection, untreated DCs showed an elevated IL-10 levels compared to *LmCen*$^{-/-}$ infection suggesting the baseline differences in the two infections (Figure 5I). Addition of FICZ increased the IL-10 levels in *LmWT* significantly more than *LmCen*$^{-/-}$ infection compared to naive treated DCs, reflecting the different underlying levels of indole-3 acetaldehyde, the substrate of FICZ in the two infections (Figure 5I).

DISCUSSION

The live attenuated *LmCen*$^{-/-}$ strain showed potent protection while maintaining the safety characteristics in pre-clinical animal models and is being developed as a candidate vaccine against leishmaniasis.[5,9] However, the mechanisms underlying the induction of protective immunity upon immunization with *LmCen*$^{-/-}$ parasites are not well understood.[55] The interaction between the host metabolism and the immune regulation that occurs in the context of an infection may provide a window to identify the mechanisms of protection and pathogenicity.

Studies of *Leishmania* infected phagocytic cells have demonstrated that metabolic changes play an important role in sustaining parasite growth through nutrient acquisition, and pathogenesis by altering of the host immune system. For example, *Leishmania* parasites are purine auxotrophs and dependent on the host's purine metabolism to scavenge purines.[56,57] In addition to nutrient acquisition, metabolic reprogramming can also alter cytokine signaling to favor parasite growth, such as the surge in mTORC1 activity in *Leishmania*-infected cells, which leads to increased glycolysis, fatty acid biosynthesis, and oxidative phosphorylation, pathways that collectively promote parasite growth.[58–60]

In addition to studies of pathogenesis, metabolomic analyses have been applied to identify immune mechanisms of protection in several vaccines. For example, metabolomic analysis to study the mechanisms of immune protection of a vaccine against *Vibrio alginolyticus* demonstrated that elevated TCA cycle activity is crucial for vaccine immunity with the intermediate metabolite, formate, increasing the transcription of the innate immune genes *il1β*, *il-8*, and *lysozyme* to promote a pro-inflammatory environment in the host.[61] Similar studies in the CoronaVac (Sinovac) vaccine against Coronavirus reported that amino acid metabolism, such as phenylalanine, glycine, serine, proline, and arginine were significantly upregulated in the vaccinated hosts and played a role in the antibody production.[62] Given the role that metabolic reprogramming plays an important role in both pathogenesis and vaccine immunity, exploring such pathways early on when the immune programming is initiated may uncover the *LmCen*$^{-/-}$ immunization induced mechanisms of protection.

The results of our pathway analysis showed that distinct metabolic pathways were enriched in the virulent *LmWT* infection compared to *LmCen*$^{-/-}$ immunization. Arginine metabolism was upregulated in both *LmWT* and *LmCen*$^{-/-}$ infections compared to naive controls with different products of arginine catabolism enriched in the two conditions. Arginine metabolism yields nitric oxide as one of its end-products that has anti-parasitic activity or polyamines such as ornithine and spermine that promote parasite growth.[15,27] Arginine metabolism can also affect the M1 and the M2 differentiation of macrophages.[27,63,64] In presence of a pro-inflammatory environment with high levels of IFN-γ, arginine metabolism leads to the synthesis of nitric oxide via nitric oxide synthase, with citrulline also being made as a byproduct that can

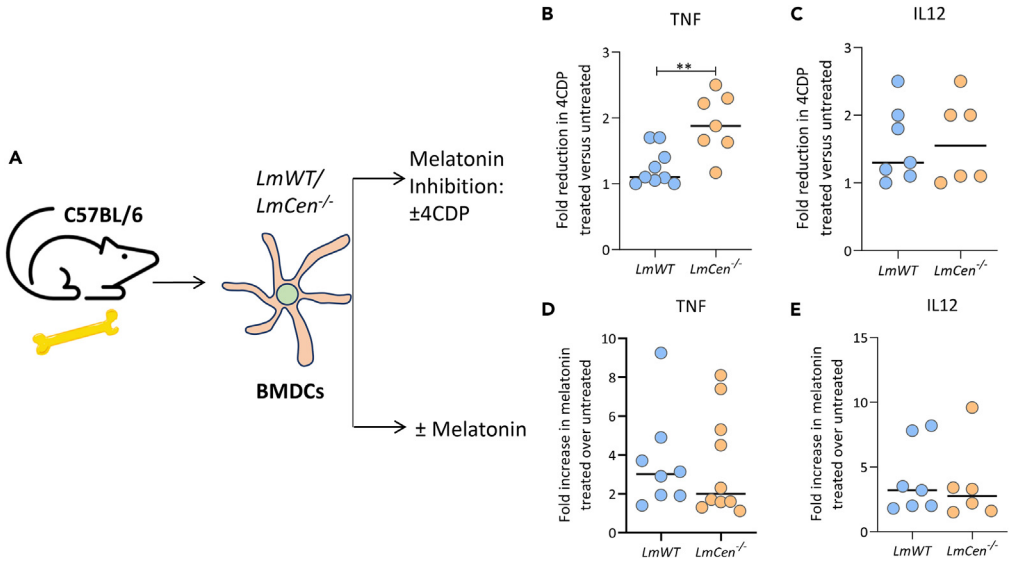

Figure 4. Validation of the role of melatonin in vaccine induced immunity

(A–E) To confirm the role of melatonin in the expression of TNF and IL-12 in *LmWT* and *LmCen*$^{-/-}$ infections, BMDCs were infected overnight with *LmWT* or *LmCen*$^{-/-}$ (A). After 24 h, 4CDP was added to the culture for an additional 24 h, and the expression levels of TNF and IL-12 were measured by RT-PCR. Treated naive BMDCs were used for calculating fold enrichment of the analytes. Upon the addition of 4-CDP, the expression of TNF was reduced in both *LmCen*$^{-/-}$ and the *LmWT* infections. The reduction in TNF was significant in *LmWT* infection compared to *LmCen*$^{-/-}$ infection (B). IL-12 levels were also reduced in both infections compared to naive upon 4CDP treatment (C). Conversely, addition of melatonin resulted an increase in TNF in both *LmCen*$^{-/-}$ and *LmWT* infections (D). Similar increase in IL-12 was also observed in both infections upon treatment with melatonin compared to naive controls (E). Data are represented as mean ± SEM. Data represents one of three experiments with N = 6–9 per group. **p < 0.01, unpaired *t* test.

be used for arginine synthesis as well.[63,64] On the other hand, under an anti-inflammatory milieu, arginase can transform arginine into ornithine as a part of the urea cycle, which eventually leads to the production of proline and polyamines.[63–65] Ornithine can be a source of nutrients for parasite; hence, elevated levels of ornithine is a characteristic of the M2 macrophages and a cellular environment that promotes the parasitic growth.[27] Consistent with these results, enrichment of ornithine in the *LmWT* infection suggests that arginine metabolism is being used to synthesize high levels of polyamines to support the parasite amplification as was reported previously.[27]

Interestingly, both *LmWT* infection and *LmCen*$^{-/-}$ immunization induced an enrichment of arginine and citrulline; however, no ornithine was detected in *LmCen*$^{-/-}$ immunization. Previous reports showed that immunization with *L. donovani centrin* deletion mutants induces significantly elevated nitric oxide production mediated by arginase1 enzyme than the virulent infection.[66,67] It is likely that arginine metabolism produces nitric oxide in *LmCen*$^{-/-}$ infection as well, however that remains to be tested. Thus, even though arginine metabolism is enriched in both the *LmWT* and the *LmCen*$^{-/-}$ infections, the products of this metabolism are distinct that either support the proliferation or clearance of the parasites. Only spermine, a downstream product of arginine metabolism, was detected in *LmCen*$^{-/-}$ infection. Interestingly, spermine has been shown to inhibit the induction of nitric oxide synthase.[68,69] Thus, the role of spermine in the *LmCen*$^{-/-}$ immunization remains to be explored.

Arginine and tryptophan metabolisms are mechanistically linked through the activities of the rate limiting enzymes Arg1 and IDO1.[44–46] Tryptophan metabolism can also affect macrophage polarization.[27,70] Tryptophan is typically catabolized via three metabolic pathways: the kynurenine, the indole, and the serotonin pathways. While the kynurenine[53,71–74] and indole pathways[74–77] typically induce anti-inflammatory and immunosuppressive effects, the serotonin pathway produces melatonin, known as an immune booster[48,78] and a vaccine-adjuvant.[79,80] Tryptophan metabolism was altered in both the *LmCen*$^{-/-}$ and the *LmWT* datasets, however, analysis of the metabolites showed that tryptophan metabolism was differentially regulated in the immunized and infected conditions as revealed by the concentrations of kynurenine, indole-3-acetaldehyde and melatonin.

In the *LmWT* infection, the kynurenine levels were highly enriched, compared to *LmCen*$^{-/-}$ immunization. Kynurenine has been the subject of much interest due to its immunomodulatory role through an interaction with the aryl hydrocarbon receptor (AhR).[52,81] In this pathway, IFN-γ strongly induces the conversion of tryptophan into kynurenine, mediated by the IDO-1 enzyme.[53,72,82] The kynurenine may then induce an immunomodulatory impact by binding to AhR.[52,83–85] Once activated upon the binding of kynurenine, AhR is translocated from the cytoplasm into the nucleus and initiates the transcription of the anti-inflammatory TGF-β and in turn causes the reduced expression of IFN-γ.[53,86] This interaction creates a positive loop which results in the increased transcription of IDO-1 and an inhibition of IFN-γ, leading to higher levels of kynurenine-AhR signaling through the elevated levels of kynurenine.[53,87]

The Kynurenine-AhR signaling has long been studied for its impact on the immune response to infections and cancer immunity.[88] For example, Kynurenine-AhR signaling has been investigated toward suppressing the anti-tumor immune response and promoting tumor

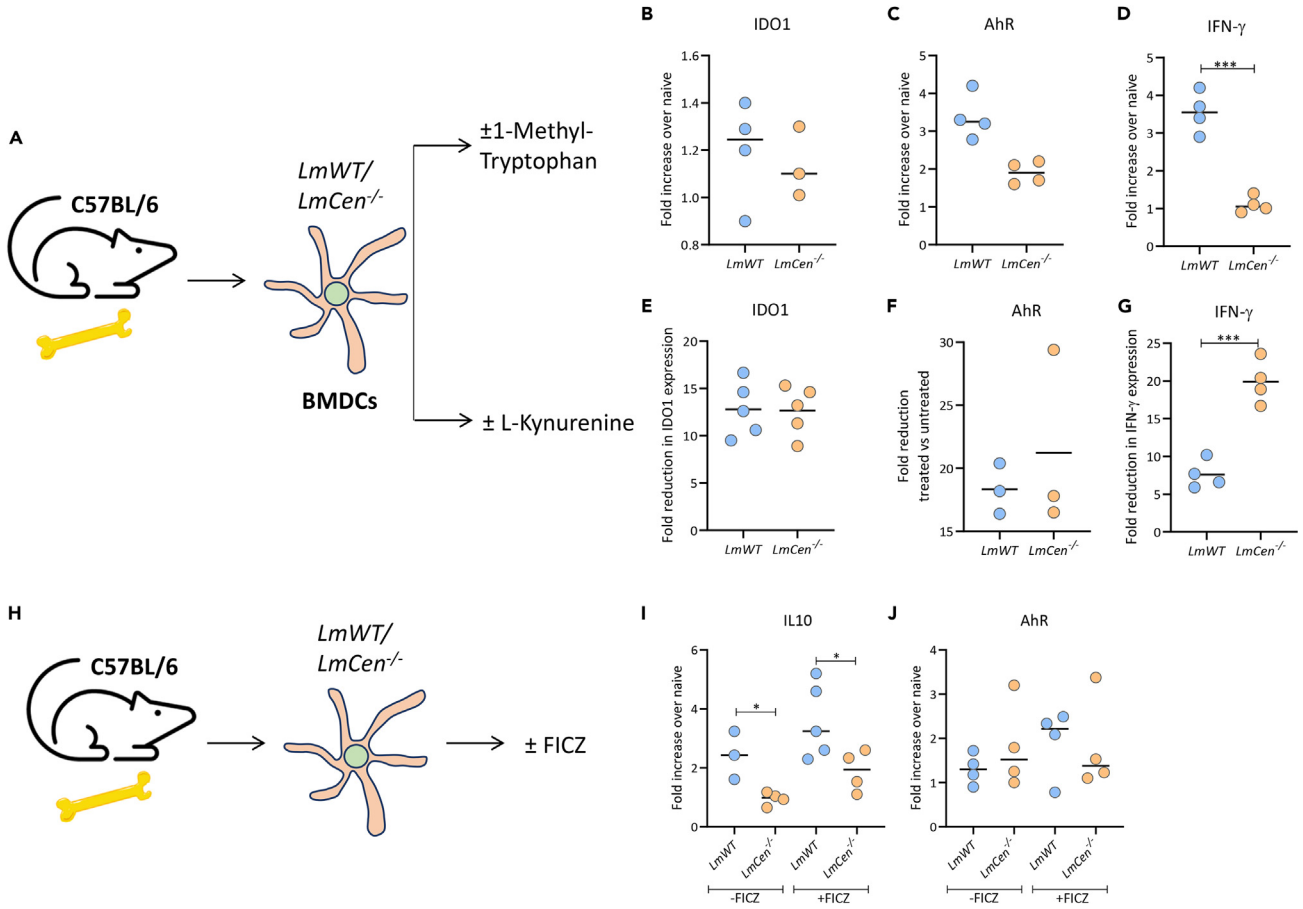

Figure 5. Validation of the role of kynurenine and FICZ in vaccine induced immunity

(A–J) To confirm kynurenine-dependent alteration of IDO-1, AhR, and IFN-γ expression in *LmWT* and *LmCen*$^{-/-}$ infections, BMDCs were infected overnight with *LmWT* or *LmCen*$^{-/-}$ (A). After 24 h, 1-methyl tryptophan or kynurenine were added, and the expression levels of IDO-1 (B), AhR (C), and IFN-γ (D) were measured by RT-PCR. Treated naive BMDCs were used for calculating fold enrichment of the analytes. Upon the addition of 1-MT, in both *LmCen*$^{-/-}$ and the *LmWT* infections, the expression of AhR (C) and IFN-γ (D) were increased. Both *LmCen*$^{-/-}$ and *LmWT* infections showed a decrease in IDO1 (E), AhR (F) and IFN-γ (G) expression upon the addition of kynurenine, showing that the expression of AhR and IFN-γ were kynurenine-dependent. To confirm the role of FICZ in the induction of IL-10, BMDCs were infected overnight with *LmWT* or *LmCen*$^{-/-}$ (H). After 24 h, FICZ was added, and the expression levels of IL-10 (I) and AhR (J) were measured by RT-PCR. Upon the addition of FICZ, in both *LmCen*$^{-/-}$ and the *LmWT* infections, the expression of IL-10 was increased (I). Both *LmCen*$^{-/-}$ and *LmWT* infections showed an increase in AhR expression (J) upon the addition of FICZ, showing that the expression of IL-10 was FICZ-dependent. Data are represented as mean ± SEM. Data represents one of three experiments with N = 3–5 per group. *p < 0.05, ***p < 0.001, unpaired t test.

growth,[89–92] yielding IDO-1 inhibitors as promising candidates for cancer therapy.[93–95] On the other hand, Kynurenine-AhR signaling has been found to generate regulatory T-cells and inhibiting the Th1 response[20,96] in viral[97–99] and parasitic[100–104] diseases, including Malaria, *Toxoplasma gondii*, and Influenza.

Previous research has shown that elevated IDO-1 expression in *L. major* infection attenuates the pro-inflammatory immune responses in a manner that leads to chronic inflammation and increased parasitic burden in the host.[11] It has also been found that the kynurenine-AhR signaling in *Leishmania*-infected dendritic cells, induced elevated generation of regulatory T-cells, inhibited IFN-γ expression, and increased levels of IL-10 signaling, creating an environment that promoted parasitic growth.[81] In agreement with these observations, our PCR data showed that the depletion of L-kynurenine by treating with 1-Methyl tryptophan, an inhibitor of IDO1,[54] increased the expression of IFN-γ, while the addition of L-kynurenine significantly inhibited the IFN-γ expression presumably by acting through AhR. Taken together, these results show that the reduction of the kynurenine levels in the *LmCen*$^{-/-}$ immunization may promote immunogenicity by inhibiting anti-inflammatory TGF-β and consequently promoting IFN-γ response.

Indole-3-acetaldehyde, another product of tryptophan metabolism was enriched in the *LmWT* infection compared to *LmCen*$^{-/-}$ infection. Indole-3-acetaldehyde is catabolized from tryptophan through an interaction in which the Interleukin-4 induced gene 1 (IL4I1) is the rate-limiting enzyme.[75–77] Indole-3-acetaldehyde can then be rearranged to form 6-formylindolo[3,2-*b*]carbazole (FICZ), another endogenous ligand of AhR.[75–77,105,106] The FICZ-AhR interaction through the transcription factor c-Maf leads to the expression of anti-inflammatory IL-10 cytokine,[107] and increased expression of IL4I1 through the transcription factor RORγt, creating an environment that supports pathogenic

growth.[74,75] The elevated levels of IL-10 observed upon exogenous addition of FICZ, the downstream product of indole-3-acetaldehyde in *LmWT* infection and to a less extent in *LmCen*$^{-/-}$ infection indicate that FICZ-AhR-*c*-Maf signaling may be responsible for the production of IL-10 that promotes pathogenicity. Reduced IL-10 levels observed in *LmCen*$^{-/-}$ compared to *LmWT* in both untreated and FICZ treated DCs suggests the differential metabolic regulation of indole-3-acetaldehyde that underlies the pro-inflammatory milieu that enables the development of protective immunity.

The serotonin pathway of tryptophan catabolism was also found to be differentially regulated in our dataset, with melatonin only being detected in the *LmCen*$^{-/-}$ immunization but not in *LmWT* infection. Melatonin is one of the main end-products of the serotonin pathway, where the rate-limiting enzyme tryptophan hydroxylase (TPH) can catalyze the conversion of tryptophan to 5-hydrxytryptophan (5-HTP) that later yields N-acetylserotonin, and serotonin.[47,48,78] Upon its release, melatonin has been shown to induce a strong-pro-inflammatory response in the host by stimulating significant IL-12 release in dendritic cells and macrophages.[48,108,109] The immune-boosting properties of melatonin have led to its usage as a vaccine adjuvant.[79,80] Reduced levels of TNF observed in both *LmWT* and *LmCen*$^{-/-}$ upon addition of 4-CDP that inhibits melatonin synthesis revealed that the endogenous pro-inflammatory activities previously reported in *LmCen*$^{-/-}$ studies might be mediated by melatonin produced by differential utilization of tryptophan in the two infections. The levels of IL-12 are not affected by the 4CDP treatment in both infections however, the levels of TNF are significantly reduced in *LmCen*$^{-/-}$ immunization compared to *LmWT* infection. Conversely addition of melatonin increased the TNF and IL-12 levels in both *LmWT* and *LmCen*$^{-/-}$ infections suggesting the potent immunoregulatory role for this metabolite in vaccine induced protective immunity. Thus, the elevated levels of melatonin observed in *LmCen*$^{-/-}$ immunization may have an endogenous adjuvant activity potentiating a strong its immune response.

Collectively, our metabolomic data indicates that the *LmCen*$^{-/-}$ immunization alters all three pathways of tryptophan catabolism toward inducing host-protective immune response. The binding of Kynurenine and/or FICZ to AhR in *LmCen*$^{-/-}$ appear to be limited due to their low abundance, while the tryptophan is mainly utilized for the production of melatonin that enhance a pro-inflammatory response.

While the metabolic analysis of *LmCen*$^{-/-}$ revealed tryptophan metabolism affecting the immune-protection, a similar metabolic analysis in the *Centrin*-deleted *L. mexicana* (*LmexCen*$^{-/-}$) strain revealed the metabolic pathways underlying immune protection are different between the two strains. *L. mexicana* is a new world *Leishmania* species that causes CL. We found that in *LmexCen*$^{-/-}$ the pentose phosphate pathway being the most highly enriched pathway of the *LmexCen*$^{-/-}$ vaccine immunization that enhanced the production of nitric oxide and IL1-β. Thus, the immunological characteristics observed in the two mutant strains may be associated with the metabolic shifts observed in the two infections. Our findings show the importance of understanding the role of metabolomics in the generation of immune responses by vaccines.

Limitations of the study

The results in Tables 1 and 2, show one of the complications of untargeted metabolomics, which is the presence of multiple isoforms of the same compound that can sometimes have opposite fold change directions and create potential ambiguity in the interpretation of the results. Additionally, the annotation of the metabolites is tentative as they are based exclusively on the formula with no additional information regarding the compound structures.

STAR★METHODS

Detailed methods are provided in the online version of this paper and include the following:

- KEY RESOURCES TABLE
- RESOURCE AVAILABILITY
  - Lead contact
  - Materials availability
  - Data and code availability
- EXPERIMENTAL MODEL AND SUBJECT DETAILS
  - Mice
  - Parasites
  - BMDCs primary culture
- METHOD DETAILS
  - *In vivo* infection
  - Parasite burden determination
  - Mass spectrometry
  - Pathway analysis of mass spectrometry data
  - Metscape analysis
  - *In vitro* cell culture and infection
- QUANTIFICATION AND STATISTICAL ANALYSIS
  - Statistical analysis of MS datasets

SUPPLEMENTAL INFORMATION

Supplemental information can be found online at https://doi.org/10.1016/j.isci.2023.107593.

ACKNOWLEDGMENTS

We gratefully acknowledge the mass spectrometry core at the Ohio State University, and Ms. Nevien Ismail at the FDA for her technical help with the animal experiments.

Our contributions are an informal communication and represent our own best judgement. These comments do not bind or obligate FDA. The work presented in this study is supported by the intramural funding from CBER/FDA to HLN.

AUTHOR CONTRIBUTIONS

G.V., S.G., H.L.N., and A.R.S. designed the experiments. G.V., T.O., N.A., P.B., and H.L.M. performed the experiments. T.O. and N.A.S.G. analyzed the mass spectrometry data. G.V. and S.G. wrote the manuscript. G.V., T.O., N.A., S.G., H.L.N., S.H., G.M., and A.R.S. revised the manuscript.

DECLARATION OF INTERESTS

The FDA is currently a co-owner of two US patents that claim attenuated *Leishmania* species with the *centrin* gene deletion (US7,887,812 and US8,877,213). This article reflects the views of the authors and should not be construed to represent FDA's views or policies. The remaining authors declare no competing interests.

Received: September 14, 2022
Revised: July 7, 2023
Accepted: August 7, 2023
Published: August 29, 2023

REFERENCES

1. Kaye, P., and Scott, P. (2011). Leishmaniasis: complexity at the host-pathogen interface. Nat. Rev. Microbiol. *9*, 604–615. https://doi.org/10.1038/nrmicro2608.
2. Torres-Guerrero, E., Quintanilla-Cedillo, M.R., Ruiz-Esmenjaud, J., and Arenas, R. (2017). Leishmaniasis: a review. F1000Res. *6*, 750. https://doi.org/10.12688/f1000research.11120.1.
3. Reithinger, R., Dujardin, J.C., Louzir, H., Pirmez, C., Alexander, B., and Brooker, S. (2007). Cutaneous leishmaniasis. Lancet Infect. Dis. *7*, 581–596. https://doi.org/10.1016/S1473-3099(07)70209-8.
4. Curtin, J.M., and Aronson, N.E. (2021). Leishmaniasis in the United States: Emerging Issues in a Region of Low Endemicity. Microorganisms *9*, 578. https://doi.org/10.3390/microorganisms9030578.
5. Zhang, W.W., Karmakar, S., Gannavaram, S., Dey, R., Lypaczewski, P., Ismail, N., Siddiqui, A., Simonyan, V., Oliveira, F., Coutinho-Abreu, I.V., et al. (2020). A second generation leishmanization vaccine with a markerless attenuated Leishmania major strain using CRISPR gene editing. Nat. Commun. *11*, 3461. https://doi.org/10.1038/s41467-020-17154-z.
6. Selvapandiyan, A., Debrabant, A., Duncan, R., Muller, J., Salotra, P., Sreenivas, G., Salisbury, J.L., and Nakhasi, H.L. (2004). Centrin gene disruption impairs stage-specific basal body duplication and cell cycle progression in Leishmania. J. Biol. Chem. *279*, 25703–25710. https://doi.org/10.1074/jbc.M402794200.
7. Fiuza, J.A., Gannavaram, S., Santiago, H.d.C., Selvapandiyan, A., Souza, D.M., Passos, L.S.A., de Mendonça, L.Z., Lemos-Giunchetti, D.d.S., Ricci, N.D., Bartholomeu, D.C., et al. (2015). Vaccination using live attenuated Leishmania donovani centrin deleted parasites induces protection in dogs against Leishmania infantum. Vaccine *33*, 280–288. https://doi.org/10.1016/j.vaccine.2014.11.039.
8. Selvapandiyan, A., Dey, R., Nylen, S., Duncan, R., Sacks, D., and Nakhasi, H.L. (2009). Intracellular replication-deficient Leishmania donovani induces long lasting protective immunity against visceral leishmaniasis. J. Immunol. *183*, 1813–1820. https://doi.org/10.4049/jimmunol.0900276.
9. Karmakar, S., Ismail, N., Oliveira, F., Oristian, J., Zhang, W.W., Kaviraj, S., Singh, K.P., Mondal, A., Das, S., Pandey, K., et al. (2021). Preclinical validation of a live attenuated dermotropic Leishmania vaccine against vector transmitted fatal visceral leishmaniasis. Commun. Biol. *4*, 929. https://doi.org/10.1038/s42003-021-02446-x.
10. Volpedo, G., Huston, R.H., Holcomb, E.A., Pacheco-Fernandez, T., Gannavaram, S., Bhattacharya, P., Nakhasi, H.L., and Satoskar, A.R. (2021). From infection to vaccination: reviewing the global burden, history of vaccine development, and recurring challenges in global leishmaniasis protection. Expert Rev. Vaccines *20*, 1431–1446. https://doi.org/10.1080/14760584.2021.1969231.
11. Makala, L.H.C., Baban, B., Lemos, H., El-Awady, A.R., Chandler, P.R., Hou, D.Y., Munn, D.H., and Mellor, A.L. (2011). Leishmania major attenuates host immunity by stimulating local indoleamine 2,3-dioxygenase expression. J. Infect. Dis. *203*, 715–725. https://doi.org/10.1093/infdis/jiq095.
12. Gupta, G., Oghumu, S., and Satoskar, A.R. (2013). Mechanisms of immune evasion in leishmaniasis. Adv. Appl. Microbiol. *82*, 155–184. https://doi.org/10.1016/B978-0-12-407679-2.00005-3.
13. Moreira, D., Rodrigues, V., Abengozar, M., Rivas, L., Rial, E., Laforge, M., Li, X., Foretz, M., Viollet, B., Estaquier, J., et al. (2015). Leishmania infantum modulates host macrophage mitochondrial metabolism by hijacking the SIRT1-AMPK axis. PLoS Pathog. *11*, e1004684. https://doi.org/10.1371/journal.ppat.1004684.
14. Murray, H.W. (1981). Susceptibility of Leishmania to oxygen intermediates and killing by normal macrophages. J. Exp. Med. *153*, 1302–1315. https://doi.org/10.1084/jem.153.5.1302.
15. Liew, F.Y., Millott, S., Parkinson, C., Palmer, R.M., and Moncada, S. (1990). Macrophage killing of Leishmania parasite in vivo is mediated by nitric oxide from L-arginine. J. Immunol. *144*, 4794–4797.
16. Guizani-Tabbane, L., Ben-Aissa, K., Belghith, M., Sassi, A., and Dellagi, K. (2004). Leishmania major amastigotes induce p50/c-Rel NF-kappa B transcription factor in human macrophages: involvement in cytokine synthesis. Infect. Immun. *72*, 2582–2589. https://doi.org/10.1128/IAI.72.5.2582-2589.2004.
17. Chandra, D., and Naik, S. (2008). Leishmania donovani infection down-regulates TLR2-stimulated IL-12p40 and activates IL-10 in cells of macrophage/monocytic lineage by modulating MAPK pathways through a contact-dependent mechanism. Clin. Exp. Immunol. *154*, 224–234. https://doi.org/10.1111/j.1365-2249.2008.03741.x.
18. Nandan, D., and Reiner, N.E. (1995). Attenuation of gamma interferon-induced tyrosine phosphorylation in mononuclear phagocytes infected with Leishmania donovani: selective inhibition of signaling

through Janus kinases and Stat1. Infect. Immun. *63*, 4495–4500. https://doi.org/10.1128/iai.63.11.4495-4500.1995.

19. Barral-Netto, M., Barral, A., Brownell, C.E., Skeiky, Y.A., Ellingsworth, L.R., Twardzik, D.R., and Reed, S.G. (1992). Transforming growth factor-beta in leishmanial infection: a parasite escape mechanism. Science *257*, 545–548. https://doi.org/10.1126/science.1636092.
20. Fallarino, F., Grohmann, U., You, S., McGrath, B.C., Cavener, D.R., Vacca, C., Orabona, C., Bianchi, R., Belladonna, M.L., Volpi, C., et al. (2006). The combined effects of tryptophan starvation and tryptophan catabolites down-regulate T cell receptor zeta-chain and induce a regulatory phenotype in naive T cells. J. Immunol. *176*, 6752–6761. https://doi.org/10.4049/jimmunol.176.11.6752.
21. Karmakar, S., Volpedo, G., Zhang, W.W., Lypaczewski, P., Ismail, N., Oliveira, F., Oristian, J., Meneses, C., Gannavaram, S., Kamhawi, S., et al. (2022). Centrin-deficient Leishmania mexicana confers protection against Old World visceral leishmaniasis. NPJ Vaccines *7*, 157. https://doi.org/10.1038/s41541-022-00574-x.
22. Volpedo, G., Pacheco-Fernandez, T., Holcomb, E.A., Zhang, W.-W., Lypaczewski, P., Cox, B., Fultz, R., Mishan, C., Verma, C., Huston, R.H., et al. (2022). Centrin-deficient Leishmania mexicana confers protection against New World cutaneous leishmaniasis. NPJ Vaccines *7*, 32. https://doi.org/10.1038/s41541-022-00449-1.
23. Pavlova, N.N., and Thompson, C.B. (2016). The Emerging Hallmarks of Cancer Metabolism. Cell Metabol. *23*, 27–47. https://doi.org/10.1016/j.cmet.2015.12.006.
24. Ward, P.S., and Thompson, C.B. (2012). Metabolic reprogramming: a cancer hallmark even warburg did not anticipate. Cancer Cell *21*, 297–308. https://doi.org/10.1016/j.ccr.2012.02.014.
25. Hu, C., Xuan, Y., Zhang, X., Liu, Y., Yang, S., and Yang, K. (2022). Immune cell metabolism and metabolic reprogramming. Mol. Biol. Rep. *49*, 9783–9795. https://doi.org/10.1007/s11033-022-07474-2.
26. O'Neill, L.A.J., Kishton, R.J., and Rathmell, J. (2016). A guide to immunometabolism for immunologists. Nat. Rev. Immunol. *16*, 553–565. https://doi.org/10.1038/nri.2016.70.
27. Naderer, T., and McConville, M.J. (2008). The Leishmania-macrophage interaction: a metabolic perspective. Cell Microbiol. *10*, 301–308. https://doi.org/10.1111/j.1462-5822.2007.01096.x.
28. Ty, M.C., Loke, P., Alberola, J., Rodriguez, A., and Rodriguez-Cortes, A. (2019). Immuno-metabolic profile of human macrophages after Leishmania and Trypanosoma cruzi infection. PLoS One *14*, e0225588. https://doi.org/10.1371/journal.pone.0225588.
29. Ganeshan, K., and Chawla, A. (2014). Metabolic regulation of immune responses. Annu. Rev. Immunol. *32*, 609–634. https://doi.org/10.1146/annurev-immunol-032713-120236.
30. Basit, F., Mathan, T., Sancho, D., and de Vries, I.J.M. (2018). Human Dendritic Cell Subsets Undergo Distinct Metabolic Reprogramming for Immune Response. Front. Immunol. *9*, 2489. https://doi.org/10.3389/fimmu.2018.02489.
31. Thwe, P.M., Pelgrom, L.R., Cooper, R., Beauchamp, S., Reisz, J.A., D'Alessandro, A., Everts, B., and Amiel, E. (2017). Cell-Intrinsic Glycogen Metabolism Supports Early Glycolytic Reprogramming Required for Dendritic Cell Immune Responses. Cell Metabol. *26*, 558–567.e5. https://doi.org/10.1016/j.cmet.2017.08.012.
32. Basit, F., and de Vries, I.J.M. (2019). Dendritic Cells Require PINK1-Mediated Phosphorylation of BCKDE1alpha to Promote Fatty Acid Oxidation for Immune Function. Front. Immunol. *10*, 2386. https://doi.org/10.3389/fimmu.2019.02386.
33. Basit, F., van Oorschot, T., van Buggenum, J., Derks, R.J.E., Kostidis, S., Giera, M., and de Vries, I.J.M. (2022). Metabolomic and lipidomic signatures associated with activation of human cDC1 (BDCA3(+)/CD141(+)) dendritic cells. Immunology *165*, 99–109. https://doi.org/10.1111/imm.13409.
34. Naderer, T., Ellis, M.A., Sernee, M.F., De Souza, D.P., Curtis, J., Handman, E., and McConville, M.J. (2006). Virulence of Leishmania major in macrophages and mice requires the gluconeogenic enzyme fructose-1,6-bisphosphatase. Proc. Natl. Acad. Sci. USA *103*, 5502–5507. https://doi.org/10.1073/pnas.0509196103.
35. Ilg, T. (2002). Generation of myo-inositol-auxotrophic Leishmania mexicana mutants by targeted replacement of the myo-inositol-1-phosphate synthase gene. Mol. Biochem. Parasitol. *120*, 151–156. https://doi.org/10.1016/s0166-6851(01)00435-2.
36. Maugeri, D.A., Cazzulo, J.J., Burchmore, R.J.S., Barrett, M.P., and Ogbunude, P.O.J. (2003). Pentose phosphate metabolism in Leishmania mexicana. Mol. Biochem. Parasitol. *130*, 117–125. https://doi.org/10.1016/s0166-6851(03)00173-7.
37. Hart, D.T., and Coombs, G.H. (1982). Leishmania mexicana: energy metabolism of amastigotes and promastigotes. Exp. Parasitol. *54*, 397–409. https://doi.org/10.1016/0014-4894(82)90049-2.
38. Rosenzweig, D., Smith, D., Opperdoes, F., Stern, S., Olafson, R.W., and Zilberstein, D. (2008). Retooling Leishmania metabolism: from sand fly gut to human macrophage. Faseb. J. *22*, 590–602. https://doi.org/10.1096/fj.07-9254com.
39. Geraldo, M.V., Silber, A.M., Pereira, C.A., and Uliana, S.R.B. (2005). Characterisation of a developmentally regulated amino acid transporter gene from Leishmania amazonensis. FEMS Microbiol. Lett. *242*, 275–280. https://doi.org/10.1016/j.femsle.2004.11.030.
40. Shaked-Mishan, P., Suter-Grotemeyer, M., Yoel-Almagor, T., Holland, N., Zilberstein, D., and Rentsch, D. (2006). A novel high-affinity arginine transporter from the human parasitic protozoan Leishmania donovani. Mol. Microbiol. *60*, 30–38. https://doi.org/10.1111/j.1365-2958.2006.05060.x.
41. Sarkar, I., Zardini Buzatto, A., Garg, R., Li, L., and van Drunen Littel-van den Hurk, S. (2019). Metabolomic and Immunological Profiling of Respiratory Syncytial Virus Infection after Intranasal Immunization with a Subunit Vaccine Candidate. J. Proteome Res. *18*, 1145–1161. https://doi.org/10.1021/acs.jproteome.8b00806.
42. Scott, P., and Novais, F.O. (2016). Cutaneous leishmaniasis: immune responses in protection and pathogenesis. Nat. Rev. Immunol. *16*, 581–592. https://doi.org/10.1038/nri.2016.72.
43. Colpitts, S.L., and Scott, P. (2010). The early generation of a heterogeneous CD4+ T cell response to Leishmania major. J. Immunol. *185*, 2416–2423. https://doi.org/10.4049/jimmunol.1000483.
44. Mondanelli, G., Bianchi, R., Pallotta, M.T., Orabona, C., Albini, E., Iacono, A., Belladonna, M.L., Vacca, C., Fallarino, F., Macchiarulo, A., et al. (2017). A Relay Pathway between Arginine and Tryptophan Metabolism Confers Immunosuppressive Properties on Dendritic Cells. Immunity *46*, 233–244. https://doi.org/10.1016/j.immuni.2017.01.005.
45. Mondanelli, G., Iacono, A., Allegrucci, M., Puccetti, P., and Grohmann, U. (2019). Immunoregulatory Interplay Between Arginine and Tryptophan Metabolism in Health and Disease. Front. Immunol. *10*, 1565. https://doi.org/10.3389/fimmu.2019.01565.
46. Crowther, R.R., and Qualls, J.E. (2020). Metabolic Regulation of Immune Responses to Mycobacterium tuberculosis: A Spotlight on L-Arginine and L-Tryptophan Metabolism. Front. Immunol. *11*, 628432. https://doi.org/10.3389/fimmu.2020.628432.
47. Hsu, C.N., and Tain, Y.L. (2020). Developmental Programming and Reprogramming of Hypertension and Kidney Disease: Impact of Tryptophan Metabolism. Int. J. Mol. Sci. *21*, 8705. https://doi.org/10.3390/ijms21228705.
48. Calvo, J.R., González-Yanes, C., and Maldonado, M.D. (2013). The role of melatonin in the cells of the innate immunity: a review. J. Pineal Res. *55*, 103–120. https://doi.org/10.1111/jpi.12075.
49. Boga, J.A., Coto-Montes, A., Rosales-Corral, S.A., Tan, D.X., and Reiter, R.J. (2012). Beneficial actions of melatonin in the management of viral infections: a new use for this "molecular handyman. Rev. Med. Virol. *22*, 323–338. https://doi.org/10.1002/rmv.1714.
50. Maestroni, G. (2020). Exogenous melatonin as potential adjuvant in anti-SarsCov2 vaccines. J. Neuroimmune Pharmacol. *15*, 572–573. https://doi.org/10.1007/s11481-020-09956-1.
51. Haskologlu, I.C., Erdag, E., Sayiner, S., Abacioglu, N., and Sehirli, A.O. (2022). Melatonin and REGN-CoV2 combination as a vaccine adjuvant for Omicron variant of SARS-CoV-2. Mol. Biol. Rep. *49*, 4061–4068. https://doi.org/10.1007/s11033-022-07419-9.
52. Mezrich, J.D., Fechner, J.H., Zhang, X., Johnson, B.P., Burlingham, W.J., and Bradfield, C.A. (2010). An interaction between kynurenine and the aryl hydrocarbon receptor can generate regulatory T cells. J. Immunol. *185*, 3190–3198. https://doi.org/10.4049/jimmunol.0903670.
53. Proietti, E., Rossini, S., Grohmann, U., and Mondanelli, G. (2020). Polyamines and Kynurenines at the Intersection of Immune Modulation. Trends Immunol. *41*, 1037–1050. https://doi.org/10.1016/j.it.2020.09.007.
54. Wirthgen, E., Leonard, A.K., Scharf, C., and Domanska, G. (2020). The Immunomodulator 1-Methyltryptophan Drives Tryptophan Catabolism Toward the Kynurenic Acid Branch. Front. Immunol. *11*,

313. https://doi.org/10.3389/fimmu.2020.00313.
55. Volpedo, G., Bhattacharya, P., Gannavaram, S., Pacheco-Fernandez, T., Oljuskin, T., Dey, R., Satoskar, A.R., and Nakhasi, H.L. (2022). The History of Live Attenuated Centrin Gene-Deleted Leishmania Vaccine Candidates. Pathogens *11*, 431. https://doi.org/10.3390/pathogens11040431.
56. Marr, J.J., Berens, R.L., and Nelson, D.J. (1978). Purine metabolism in Leishmania donovani and Leishmania braziliensis. Biochim. Biophys. Acta *544*, 360–371. https://doi.org/10.1016/0304-4165(78)90104-6.
57. Boitz, J.M., Ullman, B., Jardim, A., and Carter, N.S. (2012). Purine salvage in Leishmania: complex or simple by design? Trends Parasitol. *28*, 345–352. https://doi.org/10.1016/j.pt.2012.05.005.
58. Saunders, E.C., and McConville, M.J. (2020). Immunometabolism of Leishmania granulomas. Immunol. Cell Biol. *98*, 832–844. https://doi.org/10.1111/imcb.12394.
59. Kumar, A., Das, S., Mandal, A., Verma, S., Abhishek, K., Kumar, A., Kumar, V., Ghosh, A.K., and Das, P. (2018). Leishmania infection activates host mTOR for its survival by M2 macrophage polarization. Parasite Immunol. *40*, e12586. https://doi.org/10.1111/pim.12586.
60. Weichhart, T., Hengstschläger, M., and Linke, M. (2015). Regulation of innate immune cell function by mTOR. Nat. Rev. Immunol. *15*, 599–614. https://doi.org/10.1038/nri3901.
61. Yang, J., Yang, X.L., Su, Y.B., Peng, X.X., and Li, H. (2021). Activation of the TCA Cycle to Provide Immune Protection in Zebrafish Immunized by High Magnesium-Prepared Vibrio alginolyticus Vaccine. Front. Immunol. *12*, 739591. https://doi.org/10.3389/fimmu.2021.739591.
62. Wang, Y., Wang, X., Luu, L.D.W., Chen, S., Jin, F., Wang, S., Huang, X., Wang, L., Zhou, X., Chen, X., et al. (2022). Proteomic and Metabolomic Signatures Associated With the Immune Response in Healthy Individuals Immunized With an Inactivated SARS-CoV-2 Vaccine. Front. Immunol. *13*, 848961. https://doi.org/10.3389/fimmu.2022.848961.
63. Gogoi, M., Datey, A., Wilson, K.T., and Chakravortty, D. (2016). Dual role of arginine metabolism in establishing pathogenesis. Curr. Opin. Microbiol. *29*, 43–48. https://doi.org/10.1016/j.mib.2015.10.005.
64. Rath, M., Müller, I., Kropf, P., Closs, E.I., and Munder, M. (2014). Metabolism via Arginase or Nitric Oxide Synthase: Two Competing Arginine Pathways in Macrophages. Front. Immunol. *5*, 532. https://doi.org/10.3389/fimmu.2014.00532.
65. Iniesta, V., Carcelén, J., Molano, I., Peixoto, P.M.V., Redondo, E., Parra, P., Mangas, M., Monroy, I., Campo, M.L., Nieto, C.G., and Corraliza, I. (2005). Arginase I induction during Leishmania major infection mediates the development of disease. Infect. Immun. *73*, 6085–6090. https://doi.org/10.1128/IAI.73.9.6085-6090.2005.
66. Bhattacharya, P., Dey, R., Dagur, P.K., Kruhlak, M., Ismail, N., Debrabant, A., Joshi, A.B., Akue, A., Kukuruga, M., Takeda, K., et al. (2015). Genetically Modified Live Attenuated Leishmania donovani Parasites Induce Innate Immunity through Classical Activation of Macrophages That Direct the Th1 Response in Mice. Infect. Immun. *83*, 3800–3815. https://doi.org/10.1128/IAI.00184-15.
67. Bhattacharya, P., Ismail, N., Saxena, A., Gannavaram, S., Dey, R., Oljuskin, T., Akue, A., Takeda, K., Yu, J., Karmakar, S., et al. (2022). Neutrophil-dendritic cell interaction plays an important role in live attenuated Leishmania vaccine induced immunity. PLoS Neglected Trop. Dis. *16*, e0010224. https://doi.org/10.1371/journal.pntd.0010224.
68. Wanasen, N., and Soong, L. (2008). L-arginine metabolism and its impact on host immunity against Leishmania infection. Immunol. Res. *41*, 15–25. https://doi.org/10.1007/s12026-007-8012-y.
69. Pessenda, G., and da Silva, J.S. (2020). Arginase and its mechanisms in Leishmania persistence. Parasite Immunol. *42*, e12722. https://doi.org/10.1111/pim.12722.
70. Rodrigues, V., André, S., Maksouri, H., Mouttaki, T., Chiheb, S., Riyad, M., Akarid, K., and Estaquier, J. (2019). Transcriptional Analysis of Human Skin Lesions Identifies Tryptophan-2,3-Deoxygenase as a Restriction Factor for Cutaneous Leishmania. Front. Cell. Infect. Microbiol. *9*, 338. https://doi.org/10.3389/fcimb.2019.00338.
71. Sorgdrager, F.J.H., Naudé, P.J.W., Kema, I.P., Nollen, E.A., and Deyn, P.P.D. (2019). Tryptophan Metabolism in Inflammaging: From Biomarker to Therapeutic Target. Front. Immunol. *10*, 2565. https://doi.org/10.3389/fimmu.2019.02565.
72. Fiore, A., and Murray, P.J. (2021). Tryptophan and indole metabolism in immune regulation. Curr. Opin. Immunol. *70*, 7–14. https://doi.org/10.1016/j.coi.2020.12.001.
73. Moffett, J.R., and Namboodiri, M.A. (2003). Tryptophan and the immune response. Immunol. Cell Biol. *81*, 247–265. https://doi.org/10.1046/j.1440-1711.2003.t01-1-01177.x.
74. Gargaro, M., Pirro, M., Romani, R., Zelante, T., and Fallarino, F. (2016). Aryl Hydrocarbon Receptor-Dependent Pathways in Immune Regulation. Am. J. Transplant. *16*, 2270–2276. https://doi.org/10.1111/ajt.13716.
75. Rannug, A. (2022). 6-Formylindolo[3,2-b]carbazole, a Potent Ligand for the Aryl Hydrocarbon Receptor Produced Both Endogenously and by Microorganisms, can Either Promote or Restrain Inflammatory Responses. Front. Toxicol. *4*, 775010. https://doi.org/10.3389/ftox.2022.775010.
76. Sadik, A., Somarribas Patterson, L.F., Öztürk, S., Mohapatra, S.R., Panitz, V., Secker, P.F., Pfänder, P., Loth, S., Salem, H., Prentzell, M.T., et al. (2020). IL4I1 Is a Metabolic Immune Checkpoint that Activates the AHR and Promotes Tumor Progression. Cell *182*, 1252–1270.e34. https://doi.org/10.1016/j.cell.2020.07.038.
77. Zhang, X., Gan, M., Li, J., Li, H., Su, M., Tan, D., Wang, S., Jia, M., Zhang, L., and Chen, G. (2020). Endogenous Indole Pyruvate Pathway for Tryptophan Metabolism Mediated by IL4I1. J. Agric. Food Chem. *68*, 10678–10684. https://doi.org/10.1021/acs.jafc.0c03735.
78. Carrillo-Vico, A., Lardone, P.J., Alvarez-Sánchez, N., Rodríguez-Rodríguez, A., and Guerrero, J.M. (2013). Melatonin: buffering the immune system. Int. J. Mol. Sci. *14*, 8638–8683. https://doi.org/10.3390/ijms14048638.
79. Wang, Y.X., Yang, G.H., Zhang, L.L., Wang, J., and Wang, J.F. (2021). Melatonin as Immune Potentiator for Enhancing Subunit Vaccine Efficacy against Bovine Viral Diarrhea Virus. Vaccines *9*. https://doi.org/10.3390/vaccines9091039.
80. Zhang, R., Wang, X., Ni, L., Di, X., Ma, B., Niu, S., Liu, C., and Reiter, R.J. (2020). COVID-19: Melatonin as a potential adjuvant treatment. Life Sci. *250*, 117583. https://doi.org/10.1016/j.lfs.2020.117583.
81. Nguyen, N.T., Kimura, A., Nakahama, T., Chinen, I., Masuda, K., Nohara, K., Fujii-Kuriyama, Y., and Kishimoto, T. (2010). Aryl hydrocarbon receptor negatively regulates dendritic cell immunogenicity via a kynurenine-dependent mechanism. Proc. Natl. Acad. Sci. USA *107*, 19961–19966. https://doi.org/10.1073/pnas.1014465107.
82. Duan, Z., Duan, Y., Lei, H., Hu, N., Shi, J., Shen, D., Wang, X., and Hu, Y. (2014). Attenuation of antigenic immunogenicity by kynurenine, a novel suppressive adjuvant. Hum. Vaccines Immunother. *10*, 1295–1305. https://doi.org/10.4161/hv.28099.
83. Head, J.L., and Lawrence, B.P. (2009). The aryl hydrocarbon receptor is a modulator of anti-viral immunity. Biochem. Pharmacol. *77*, 642–653. https://doi.org/10.1016/j.bcp.2008.10.031.
84. Clement, C.C., D'Alessandro, A., Thangaswamy, S., Chalmers, S., Furtado, R., Spada, S., Mondanelli, G., Ianni, F., Gehrke, S., Gargaro, M., et al. (2021). 3-hydroxy-L-kynurenamine is an immunomodulatory biogenic amine. Nat. Commun. *12*, 4447. https://doi.org/10.1038/s41467-021-24785-3.
85. Grohmann, U., and Puccetti, P. (2015). The Coevolution of IDO1 and AhR in the Emergence of Regulatory T-Cells in Mammals. Front. Immunol. *6*, 58. https://doi.org/10.3389/fimmu.2015.00058.
86. Stockinger, B., Di Meglio, P., Gialitakis, M., and Duarte, J.H. (2014). The aryl hydrocarbon receptor: multitasking in the immune system. Annu. Rev. Immunol. *32*, 403–432. https://doi.org/10.1146/annurev-immunol-032713-120245.
87. Munn, D.H., and Mellor, A.L. (2013). Indoleamine 2,3 dioxygenase and metabolic control of immune responses. Trends Immunol. *34*, 137–143. https://doi.org/10.1016/j.it.2012.10.001.
88. Stevens, E.A., Mezrich, J.D., and Bradfield, C.A. (2009). The aryl hydrocarbon receptor: a perspective on potential roles in the immune system. Immunology *127*, 299–311. https://doi.org/10.1111/j.1365-2567.2009.03054.x.
89. Opitz, C.A., Litzenburger, U.M., Sahm, F., Ott, M., Tritschler, I., Trump, S., Schumacher, T., Jestaedt, L., Schrenk, D., Weller, M., et al. (2011). An endogenous tumour-promoting ligand of the human aryl hydrocarbon receptor. Nature *478*, 197–203. https://doi.org/10.1038/nature10491.
90. Prendergast, G.C. (2011). Cancer: Why tumours eat tryptophan. Nature *478*, 192–194. https://doi.org/10.1038/478192a.
91. Xue, P., Fu, J., and Zhou, Y. (2018). The Aryl Hydrocarbon Receptor and Tumor Immunity. Front. Immunol. *9*, 286. https://doi.org/10.3389/fimmu.2018.00286.
92. Günther, J., Fallarino, F., Fuchs, D., and Wirthgen, E. (2020). Editorial: Immunomodulatory Roles of Tryptophan Metabolites in Inflammation and Cancer.

Front. Immunol. *11*, 1497. https://doi.org/10.3389/fimmu.2020.01497.

93. Zhai, L., Spranger, S., Binder, D.C., Gritsina, G., Lauing, K.L., Giles, F.J., and Wainwright, D.A. (2015). Molecular Pathways: Targeting IDO1 and Other Tryptophan Dioxygenases for Cancer Immunotherapy. Clin. Cancer Res. *21*, 5427–5433. https://doi.org/10.1158/1078-0432.CCR-15-0420.
94. Vacchelli, E., Aranda, F., Eggermont, A., Sautès-Fridman, C., Tartour, E., Kennedy, E.P., Platten, M., Zitvogel, L., Kroemer, G., and Galluzzi, L. (2014). Trial watch: IDO inhibitors in cancer therapy. OncoImmunology *3*, e957994. https://doi.org/10.4161/21624011.2014.957994.
95. Diray-Arce, J., Angelidou, A., Jensen, K.J., Conti, M.G., Kelly, R.S., Pettengill, M.A., Liu, M., van Haren, S.D., McCulloch, S.D., Michelloti, G., et al. (2022). Bacille Calmette-Guerin vaccine reprograms human neonatal lipid metabolism in vivo and in vitro. Cell Rep. *39*, 110772. https://doi.org/10.1016/j.celrep.2022.110772.
96. Campesato, L.F., Budhu, S., Tchaicha, J., Weng, C.H., Gigoux, M., Cohen, I.J., Redmond, D., Mangarin, L., Pourpe, S., Liu, C., et al. (2020). Blockade of the AHR restricts a Treg-macrophage suppressive axis induced by L-Kynurenine. Nat. Commun. *11*, 4011. https://doi.org/10.1038/s41467-020-17750-z.
97. Fox, J.M., Sage, L.K., Huang, L., Barber, J., Klonowski, K.D., Mellor, A.L., Tompkins, S.M., and Tripp, R.A. (2013). Inhibition of indoleamine 2,3-dioxygenase enhances the T-cell response to influenza virus infection. J. Gen. Virol. *94*, 1451–1461. https://doi.org/10.1099/vir.0.053124-0.
98. Adu-Gyamfi, C.G., Savulescu, D., George, J.A., and Suchard, M.S. (2019). Indoleamine 2, 3-Dioxygenase-Mediated Tryptophan Catabolism: A Leading Star or Supporting Act in the Tuberculosis and HIV Pas-de-Deux? Front. Cell. Infect. Microbiol. *9*, 372. https://doi.org/10.3389/fcimb.2019.00372.
99. Mehraj, V., and Routy, J.P. (2015). Tryptophan Catabolism in Chronic Viral Infections: Handling Uninvited Guests. Int. J. Tryptophan Res. *8*, 41–48. https://doi.org/10.4137/IJTR.S26862.
100. Dos Santos, R.O., da Cruz, M.G.S., Lopes, S.C.P., Oliveira, L.B., Nogueira, P.A., Lima, E.S., Soares, I.S., Kano, F.S., de Carvalho, A.T., Costa, F.T.M., et al. (2020). A First Plasmodium vivax Natural Infection Induces Increased Activity of the Interferon Gamma-Driven Tryptophan Catabolism Pathway. Front. Microbiol. *11*, 400. https://doi.org/10.3389/fmicb.2020.00400.
101. Schmidt, S.V., and Schultze, J.L. (2014). New Insights into IDO Biology in Bacterial and Viral Infections. Front. Immunol. *5*, 384. https://doi.org/10.3389/fimmu.2014.00384.
102. Majumdar, T., Sharma, S., Kumar, M., Hussain, M.A., Chauhan, N., Kalia, I., Sahu, A.K., Rana, V.S., Bharti, R., Haldar, A.K., et al. (2019). Tryptophan-kynurenine pathway attenuates beta-catenin-dependent pro-parasitic role of STING-TICAM2-IRF3-IDO1 signalosome in Toxoplasma gondii infection. Cell Death Dis. *10*, 161. https://doi.org/10.1038/s41419-019-1420-9.
103. Colvin, H.N., and Joice Cordy, R. (2020). Insights into malaria pathogenesis gained from host metabolomics. PLoS Pathog. *16*, e1008930. https://doi.org/10.1371/journal.ppat.1008930.
104. Cordy, R.J., Patrapuvich, R., Lili, L.N., Cabrera-Mora, M., Chien, J.T., Tharp, G.K., Khadka, M., Meyer, E.V., Lapp, S.A., Joyner, C.J., et al. (2019). Distinct amino acid and lipid perturbations characterize acute versus chronic malaria. JCI Insight *4*, e125156. https://doi.org/10.1172/jci.insight.125156.
105. Rannug, A., Rannug, U., Rosenkranz, H.S., Winqvist, L., Westerholm, R., Agurell, E., and Grafström, A.K. (1987). Certain photooxidized derivatives of tryptophan bind with very high affinity to the Ah receptor and are likely to be endogenous signal substances. J. Biol. Chem. *262*, 15422–15427.
106. Rannug, U., Rannug, A., Sjöberg, U., Li, H., Westerholm, R., and Bergman, J. (1995). Structure elucidation of two tryptophan-derived, high affinity Ah receptor ligands. Chem. Biol. *2*, 841–845. https://doi.org/10.1016/1074-5521(95)90090-x.
107. Apetoh, L., Quintana, F.J., Pot, C., Joller, N., Xiao, S., Kumar, D., Burns, E.J., Sherr, D.H., Weiner, H.L., and Kuchroo, V.K. (2010). The aryl hydrocarbon receptor interacts with c-Maf to promote the differentiation of type 1 regulatory T cells induced by IL-27. Nat. Immunol. *11*, 854–861. https://doi.org/10.1038/ni.1912.
108. Cutolo, M., Villaggio, B., Candido, F., Valenti, S., Giusti, M., Felli, L., Sulli, A., and Accardo, S. (1999). Melatonin influences interleukin-12 and nitric oxide production by primary cultures of rheumatoid synovial macrophages and THP-1 cells. Ann. N. Y. Acad. Sci. *876*, 246–254. https://doi.org/10.1111/j.1749-6632.1999.tb07645.x.
109. Lissoni, P. (1999). The pineal gland as a central regulator of cytokine network. Neuroendocrinol. Lett. *20*, 343–349.
110. Pang, Z., Zhou, G., Ewald, J., Chang, L., Hacariz, O., Basu, N., and Xia, J. (2022). Using MetaboAnalyst 5.0 for LC-HRMS spectra processing, multi-omics integration and covariate adjustment of global metabolomics data. Nat. Protoc. *17*, 1735–1761. https://doi.org/10.1038/s41596-022-00710-w.
111. Xia, J., Psychogios, N., Young, N., and Wishart, D.S. (2009). MetaboAnalyst: a web server for metabolomic data analysis and interpretation. Nucleic Acids Res. *37*, W652–W660. https://doi.org/10.1093/nar/gkp356.
112. Karnovsky, A., Weymouth, T., Hull, T., Tarcea, V.G., Scardoni, G., Laudanna, C., Sartor, M.A., Stringer, K.A., Jagadish, H.V., Burant, C., et al. (2012). Metscape 2 bioinformatics tool for the analysis and visualization of metabolomics and gene expression data. Bioinformatics *28*, 373–380. https://doi.org/10.1093/bioinformatics/btr661.
113. Kanehisa, M., Goto, S., Sato, Y., Furumichi, M., and Tanabe, M. (2012). KEGG for integration and interpretation of large-scale molecular data sets. Nucleic Acids Res. *40*, D109–D114. https://doi.org/10.1093/nar/gkr988.
114. Krämer, A., Green, J., Pollard, J., Jr., and Tugendreich, S. (2014). Causal analysis approaches in Ingenuity Pathway Analysis. Bioinformatics *30*, 523–530. https://doi.org/10.1093/bioinformatics/btt703.
115. Wohlgemuth, G., Haldiya, P.K., Willighagen, E., Kind, T., and Fiehn, O. (2010). The Chemical Translation Service–a web-based tool to improve standardization of metabolomic reports. Bioinformatics *26*, 2647–2648. https://doi.org/10.1093/bioinformatics/btq476.
116. The University of Manchester, and MIB Biospec Group Laboratory Guide for Metabolomic Experiments. www.biospec.net/wordpress/wp-content/uploads/Metabolomics-laboratory-handbook.pdf.
117. Lacerda, C.M.R., Kisiday, J., Johnson, B., and Orton, E.C. (2012). Local serotonin mediates cyclic strain-induced phenotype transformation, matrix degradation, and glycosaminoglycan synthesis in cultured sheep mitral valves. Am. J. Physiol. Heart Circ. Physiol. *302*, H1983–H1990. https://doi.org/10.1152/ajpheart.00987.2011.
118. Kiyomatsu-Oda, M., Uchi, H., Morino-Koga, S., and Furue, M. (2018). Protective role of 6-formylindolo[3,2-b]carbazole (FICZ), an endogenous ligand for arylhydrocarbon receptor, in chronic mite-induced dermatitis. J. Dermatol. Sci. *90*, 284–294. https://doi.org/10.1016/j.jdermsci.2018.02.014.

STAR★METHODS

KEY RESOURCES TABLE

REAGENT or RESOURCE	SOURCE	IDENTIFIER
Chemicals, peptides, and recombinant proteins		
Liberase-TL	Roche	Cat.No. 5401020001
DL-Kynurenine	Sigma Aldrich	Cat. No. 61250
1-Methyl-D-Tryptophan	Tocris	Cat. No. 5698
Melatonin	Sigma Aldrich	Cat. No. M5250-1G
4-Chloro-DL-Phenylalanine (4-CDP)	Sigma Aldrich	Cat. No. C6506-5G
IL-10 TaqMan Gene Expression Assay	Thermo Fisher Scientific	Mm00439614_m1
AhR TaqMan Gene Expression Assay	Thermo Fisher Scientific	Mm00478932_m1
IDO-1 TaqMan Gene Expression Assay	Thermo Fisher Scientific	Mm00492590_m1
IFN-g TaqMan Gene Expression Assay	Thermo Fisher Scientific	Mm01168134_m1
IL-12b TaqMan Gene Expression Assay	Thermo Fisher Scientific	Mm00434174_m1
TNF-a TaqMan Gene Expression Assay	Thermo Fisher Scientific	Mm00443258_m1
GAPDH TaqMan Gene Expression Assay	Thermo Fisher Scientific	Mm99999915_g1
FICZ	Sigma Aldrich	Cat. No. SML1489
IL-4	Prospec	Cat. No. cyt-282-b
GMCSF	Prospec	Cat. No. cyt-222-b
Critical commercial assays		
Applied Biosystems High Capacity cDNA Reverse Transcription Kit	Thermo Fisher Scientific	Ref. No. 4368814
TaqMan Gene Expression Master Mix	Thermo Fisher Scientific	Ref. No. 4369016
Experimental models: Organisms/strains		
Leishmania major Cen$^{-/-}$	Zhang et al.[5]	*LmCen*$^{-/-}$ derived from the parental *L. major* Friedlin (FV9) strain
Leishmania major WT	N/A	*L. major* Friedlin (FV9)
Software and algorithms		
MetaboAnalyst 4.0	Xia et al.[110,111]	MetaboAnalyst; RRID: SCR_015539
Metscape	Karnovsky et al.[112]	MetScape 3 (ncibi.org); RRID: SCR_014687
Kyoto Encyclopedia of Genetics and Genomes (KEGG)	Kanehisa et al.[113]	KEGG: Kyoto Encyclopedia of Genes and Genomes; RRID: SCR_001120
Graphpad Prism 9	Dotmatics	Home - GraphPad; RRID: SCR_002798
Ingenuity Pathway Analysis (IPA)	Kramer et al.[114]	Ingenuity Pathway Analysis | QIAGEN Digital Insights; RRID: SCR_008653
The Chemical Translation Service (CTS)	Wohlgemuth et al.[115]	CTS Proxy (ucdavis.edu)

RESOURCE AVAILABILITY

Lead contact

Further information and requests for resources and reagents should be directed to and will be fulfilled by the Lead Contact, Dr. Sreenivas Gannavaram (Sreenivas.gannavaram@fda.hhs.gov).

Materials availability

This study did not generate new unique reagents.

Data and code availability

- All relevant data is available in the main text and supplementary information. Any additional information can be provided upon reasonable request to the authors.
- This paper does not report original code.
- Any additional information required to reanalyze the data reported in this paper is available from the lead contact upon request.

EXPERIMENTAL MODEL AND SUBJECT DETAILS

Mice

The animal protocol for this study has been approved by the Institutional Animal Care and Use Committee at the Center for Biologics Evaluation and Research, US Food and Drug Administration (FDA) (ASP 1995#26). In addition, the animal protocol is in full accordance with "The guide for the care and use of animals as described in the US Public Health Service policy on Humane Care and Use of Laboratory Animals 2015." Female C57Bl/6 were purchased from Jackson Laboratories Bar Harbor, ME, USA, and were housed in the FDA animal facilities in cages shared by three mice. All the experiments were performed using 3 age-matched 6–8 week old female mice per group, randomly assigned to experimental groups. We used 3 experimental groups: 1) Naive: non-infected mice serving as controls; 2) *LmWT:* mice infected with *L. major;* and 3) *LmCen−/−:* mice infected with *L. major Cen*$^{-/-}$ mutant parasites.

Parasites

LmCen$^{-/-}$ have been previously generated by the deletion of the Centrin gene using CRISPR technology.[5] *L. major* Friedlin (FV9) parasites were routinely passaged by inoculation into the footpads of BALB/c mice. *L. major* parasites isolated from infected lesions were cultured at 27°C in M199 medium with a pH of 7.4 (Gibco, Thermo Fisher Scientific, Waltham, MA) supplemented with 10% heat-inactivated fetal bovine serum, 40 mM HEPES ((4-(2-hydroxyethyl)-1-piperazineethanesulfonic acid) (pH 7.4), 0.1 mM adenine, 5 mg/L hemin, 1 mg/L biotin, 1 mg/L biopterin, 50 U/ml penicillin, and 50 μg/ml streptomycin.

BMDCs primary culture

Bone marrow-derived Dendritic Cells (BMDCs) were obtained from the femurs of C57Bl/6 mice by flushing 3 mL of RPMI medium through the bone. After isolation, the bone marrow cell suspension was washed twice with RPMI medium and was cultured in 6-well plates, at a concentration of 2.0 x 10^6 cells per well, with RPMI medium supplemented with 10% fetal bovine serum (FBS), 1% penicillin/streptomycin, IL-4, and GM-CSF at 37°C with 5% CO_2 for 7 days until differentiation was complete.

METHOD DETAILS

In vivo infection

C57Bl/6 mice (n ≥ 4 per group) that were age matched were inoculated intradermally in the ear dermis with 1×10^6 *L major* or *LmCen*$^{-/-}$ promastigotes in the stationary phase in 10 μL PBS. After 7 days, the ipsilateral and contralateral infected ears and the naive ears were collected and processed for mass spectrometry.

Parasite burden determination

Seven days post-infection, the ears and the draining lymph nodes (dLN) from *LmWT* or *LmCen*$^{-/-}$ infected mice were harvested and processed to obtain single cell suspensions. dLNs were disaggregated using a 70 μm strainer, whereas infected ears were digested with liberase-TL (Roche Diagnostics, 0.2 mg/ml, 90 min at 37°C in 5% CO_2 incubator) followed by tissue disruption in a Medicon device (BD Biosciences). The single cell suspensions of ears and lymph nodes were cultured in 96 well plates in 1:10 serial dilutions using complete M199 media. Parasites were allowed to grow for 14 days, and the maximum dilution (log titer) where the parasites were observed (limiting dilution method) was reported.

Mass spectrometry

The ear tissue was collected, snap frozen, and processed for mass spectrometry analysis according to SOP 7 of the Laboratory Guide for Metabolomics Experiments.[116] Samples were then incubated with 500 μL of 100% MeOH and sonicated. The tissue was weighed and homogenized at 40 mg/mL of 50% MeOH solution for 3 cycles in a homogenizer with Precellys. The supernatant was collected, dried down, and reconstituted in half of the original volume in 5% MeOH with 0.1% formic acid.

Untargeted analysis was performed on a Thermo Orbitrap LTQ XL with HPLC separation on a Poroshell 120 SB-C18 (2 × 100 mm, 2.7 μm particle size) with an WPS 3000 LC system. The gradient consisted of solvent A, H2O with 0.1% Formic acid, and solvent B 100% acetonitrile at a 200 μL/min flow rate with an initial 2% solvent B with a linear ramp to 95% B at 15 min, holding at 95% B for 1 min, and back to 2% B from 16 min and equilibration of 2% B until min 32. For each sample, 5μL were injected and the top 5 ions were selected for data dependent analysis with a 15 s exclusion window.

For feature selection in the untargeted results analysis, including database comparison and statistical processing, samples were analyzed in Progenesis QI, and the pooled sample runs were selected for feature alignment. Anova p value scores between the groups were calculated

with a cutoff of <0.05. With database matching using the [Human Metabolome Database], selecting for adducts M + H, M + Na, M + K, and M+2H and less than 10 ppm mass error, unique features were tentatively identified as potential metabolites.

Pathway analysis of mass spectrometry data

We have used two different techniques in order to identify enriched pathways in our datasets. First, we used the Functional Analysis Module (MS peaks to pathways) in MetaboAnalyst 5.0[110,111]. Detected peaks (mass-to-charge ratios + retention times) from positive and negative analytical modes of the mass spectrometer for each sample were organized into four column lists along with calculated p values and t-scores from univariate t-tests. These peak list profiles were uploaded to the functional analysis module and passed the internal data integrity checks. The ion mode in MetaboAnalyst was set to the appropriate type depending on the analytical mode that was used to generate the data. For each analysis the mass tolerance was set to 10 ppm, the retention time units were set to minutes, and the option to enforce primary ions was checked. In parameter settings, the mummichog algorithm (version 2.0) and the modified gene set enrichment algorithm were used for all analyses. The p value cutoff for the mummichog algorithm was left at the default (top 10% of peaks). Currency metabolites and adducts were left at default settings. Lastly, the Kyoto Encyclopedia of Genes and Genomes (KEGG)[113] pathway library for *Mus musculus* was selected as the metabolic network that the functional analysis module would use to infer pathway activity and predict metabolite identity; only pathways/metabolite sets with at least three entries were allowed.

To confirm the enriched pathways identified with MetaboAnalyst, we also used the Ingenuity Pathway Analysis (IPA) software.[114] Metabolite matches to the detected peaks from database searches (HMDB and LIPID MAPS), along with calculated p values and fold changes were uploaded into IPA software for core analysis. The reference set was selected as the Ingenuity Knowledge Base (endogenous chemicals only) and direct and indirect relationships were considered during analysis. Settings in the networks, node type, data sources, confidence, and mutations tabs were left at default values. The species tab settings were set to mouse and uncategorized (selecting uncategorized species for metabolomics is necessary in IPA as most metabolites are not unique to any one species). Lastly, in the tissues and cell lines tab all tissues were considered in the analysis, whereas all cell lines were excluded from consideration. The p value cutoff for every analysis was set as 0.05 and the fold change cutoffs were adjusted to obtain between 200 and 1000 analysis-ready molecules and then kept the same across different analyses.

Metscape analysis

The Metscape 3.1.3 App[112] from the Cytoscape 3.9.1 software was used in order to build integrative network analysis of our *in vivo* dataset using Metscape's internal database which incorporates KEGG and EHMN data. The IDs of the metabolomic dataset were converted from HMDB IDs to KEGG IDs recognized by the Cytoscape software via the Chemical Translation Service (CTS)[115] and verified by the Metaboanalyst Compound ID Conversion tool. The metabolomic dataset was then uploaded as a compound file to Metscape and the P. Value and FC Ratio cutoff points were set at 0.05 and 1.0 respectively. A Compound-gene network was created for Tryptophan Metabolism detected in our dataset, allowing us to visualize the integrated relationship among the metabolites and genes involved in this pathway.

In vitro cell culture and infection

Bone marrow-derived Dendritic Cells (BMDCs) were obtained from the femurs of C57Bl/6 mice. After isolation, the bone marrow cell suspension was cultured in 6-well plates, at a concentration of $2.0x10^6$ cells per well, with complete RPMI medium supplemented with IL-4 and GM-CSF at 37°C with 5% CO_2 for 7 days until differentiation was complete. The differentiated BMDCs were then infected overnight with stationary phase *LmCen*$^{-/-}$ promastigotes at a 1:10 ratio of DCs to parasites, while the naive controls were treated with complete RPMI media alone. The next day, the extracellular parasites were removed by washing with PBS and new media was applied. Infected DCs and controls were treated with 600 μM of 1-methyl tryptophan (L-isomer, Sigma-Aldrich)[53] or 50 μM of kynurenine (L-isomer, Sigma-Aldrich) or melatonin (50 ng/ml, Sigma-Aldrich)[108] or 4-Cyano-4-[(dodecylsulfanylthiocarbonyl)sulfanyl]pentanoic acid(4-CDP) (10 μM, Sigma-Aldrich)[117] or 6-formylindolo[3,2-*b*]carbazole (FICZ) (5 mM, Sigma-Aldrich).[118] After a 24hrs incubation, the cells were scraped from the wells for RNA extraction and RT-PCR for the indicated genes.

QUANTIFICATION AND STATISTICAL ANALYSIS

All *in vitro* and *in vivo* data show a representative experiment with $N \geq 3$ per group. N represents different biological replicates. For the nitric oxide assay, unpaired two-tailed Mann-Whitney t test was performed using Graph Pad Prism 9 to compare statistical significance. A p value <0.05 was considered significant. In all figures * represents $p \leq 0.05$, ** represents $p \leq 0.01$ and *** represents $p \leq 0.001$ (also found in the figure legends). Error bars represent SEM (standard error of the mean).

Statistical analysis of MS datasets

For the mass spectrometry data all statistical analysis were performed with MetaboAnalyst software. Peak intensity data tables from the mass spectrometry experiment were formatted into comma-separated values (CSV) files conforming to MetaboAnalyst's requirements and uploaded into the one-factor statistical analysis module. Each analysis passed MetaboAnalyst's internal data integrity check and additional data filtering was performed based on interquartile range. On the normalization overview page, sample normalization was

performed based on the median of the data and the auto-scaling option was chosen to perform data scaling; No transformation of the data was performed. For dimensionality reduction, both principal component analysis (PCA) and partial least-squares discriminant analysis (PLS-DA) were employed. Cross-validated sum of squares (Q2) performance measures were used to determine if PLS-DA models were overfitted. Visualization of significant, differentially regulated metabolites was done by generating volcano plots with cutoffs of <0.05 false-discovery rate (FDR) and >2-fold change (FC). Clustering of samples and features were analyzed by creating dendrograms and hierarchical heatmaps, respectively.